Universitetet i Stavanger

FACULTY OF SCIENCE AND TECHNOLOGY

MASTER'S THESIS

Study programme/specialisation: Petroleum Engineering - Master of Science Degree Programme/ Reservoir Engineering	Spring semester, 2018 Open
Author: **Tina Trang Nguyen**	…… (signature of author)

Programme coordinator:

Supervisor(s): **Rune Wiggo Time, Steinar Evje**

Title of master's thesis:

Numerical and analytical analysis of flow in stratified heterogeneous porous media.

Credits: 30

Keywords: *One-dimension flow* *Boussinesq equation* *Flow in porous media* *Fissurized porous medium* *Double-porosity model*	Number of pages: 78 +supplemental material/other: Stavanger, 04.06.2018

Numerical and analytical analysis of flow in stratified heterogeneous porous media.

Master of Reservoir Engineering

Tina Trang Nguyen

Department of Petroleum Engineering
University of Stavanger
Norway
Spring 2018

Acknowledgements

First of all I would like to thank my supervisors Rune Wiggo Time and Steinar Evje for all your help and useful feedback. I would also like to thank Yang Yang Qiao for the accompanying help and support.

Thanks to my friends and family for your everlasting support and patience.

Tina Trang Nguyen,
May 2018.

Abstract

The groundwater flow through a porous media is well-researched to extend the basic knowledge in both academia and industry, specially the oil industry. The Boussinesq equation represents a water height of fluid spreads into the semi-infinite medium for unsteady flow. Property of this flow represents a groundwater flow after a high water period or after a breakthrough of a dam around a reservoir. The fluid is drained out as an intense pulse at the boundary and flow through the porous medium by gravity-driven motion. In this studying, the Boussinesq equation is re-produced from Barenblatt et al. (1999) [1]. The analytical and numerical analysis is used to solve this equation for a homogeneous porous medium. In the real life, we do not always have the homogeneous porous medium. A system fissures is counted into the Boussinesq equation and applies a basic of a "double-porosity" model for a stratified heterogeneous porous medium. The model is a system of two equations: one for water level in fissurized porous blocks and one for water level in system cracks. These equations are only solved with numerically because they are very complicated when we solve with analytically. For comparison, a purely porous blocks is obtained under same conditions with fissurized porous blocks. This demonstrates how the fissures influence on the groundwater flow in stratified heterogeneous porous media, increasing of the speed and the penetration of the fluid into the medium. At first stage, the groundwater flow is rapid breakthrough at the boundary into the porous media via a system cracks; and at later stage, the fissures is supported by the fluid in fissurized porous blocks.

Contents

1 Introduction

Flow in porous media is a subject that has been researched during over last decades extensively. Understanding this basic knowledge, we can solve problems that happen on subsurface and improve the oil industry. One of the reasons is the invention of the computer and advances information technology. A mathematical model which is derived from the physics and a massive resources gathering from the ground and sea, can simulate on a computer. This helps us to understand the complicated physical processes and combine the different resources more effectively.

In a homogeneous porous media, the water height of the groundwater flow $h(x,t)$ (figure 2A) is described by Boussinesq in 1903 [2]. The flow motion is gravity-driven by the converted mass of the fluid. A source for the mass is from a pulse breakthrough at the boundary in a very short time interval $t = \tau$ (figure 1). After that, the Boussinesq equation represents

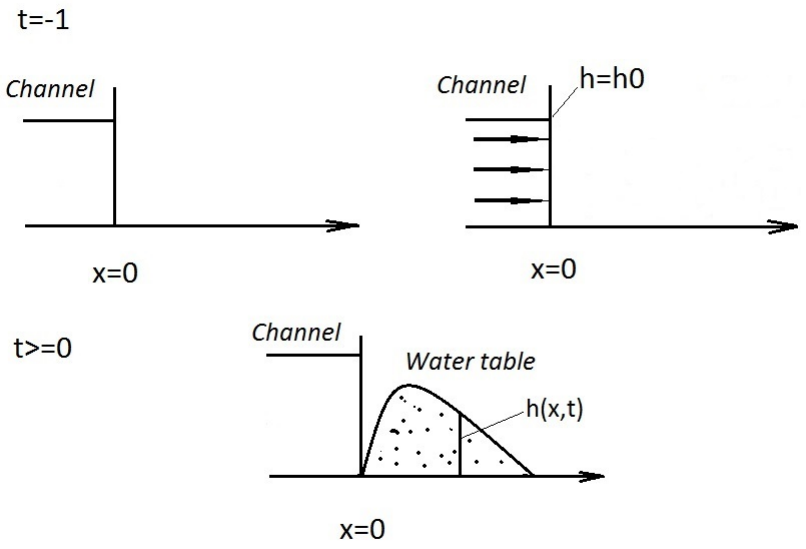

Figure 1: A sketch represents an intense pulse at the boundary in a short time interval $t = \tau \in [-1, 0]$. From the initial moment $t = -1$, groundwater flow increases rapidly to maximum water level $h = h_0$ and decreases to the initial distribution at $t = 0$.

at groundwater flow extents the fluid into the porous media at large times $t = T \gg \tau$. Analysis and numeric computations of the model show that an asymptotic solution of groundwater mound is lower with time and the front

penetrates further into the porous media.

The aim of this studying is how the groundwater flow in a stratified heterogeneous media varies from a homogeneous porous media with the same intense pulse at the boundary. Groundwater flow in which one of these medium moves faster and larger in mass of fluid. Stratified porous medium behavior is two different media that are involved in the flow process: a higher permeability medium that produces fluid extension and a lower permeability medium that recharges the higher permeability medium [3].

A mathematical model of the 'double' porous medium is 'double-porosity' model, which is derived from Barenblatt et al. (1960 & 1990) [4], [5]. The model needs to take into an exchange flow from fissurized porous blocks and a system cracks. There are two water level for fissurized porous blocks $h_B(x,t)$ and a system cracks $h_C(x,t)$ (figure 2B). These system equations are simulated in dimensionless form. The numerical results are compared with a purely porous blocks under same conditions to answer the questions above.

Outline

Chapter 2: Flow in homogeneous porous media. In this chapter, we go through the basics of flow in a porous media. We go through some background of the physics, and then derive the Boussinesq equation for water level for a homogeneous porous medium. The topic of fractures is more or less left out from the discussions in this chapter. The analytical solution of the Boussinesq equation was derived from different references. The Boussinesq equation is solved here by analytically and numerically. The problem is simulated by developing a matlab code. The results are given in figures show that the different water height of saturated region with different time.

Chapter 3: Flow in stratified heterogeneous porous media. Here, we discuss the effects of adding fissures to a porous media. We reproduce the double-porosity model for the fissurized porous medium from [1]. The model is only solved numerically from a matlab code. The results is compared to the homogeneous porous media and see how the fissures effects on the flow in porous media.

Chapter 4: Comparison on the results in purely and fissurized porous medium A purely porous blocks is computed under same conditions with fissurized porous blocks in chapter 3. At the same time, the mass of fluid and front position of groundwater flow in purely porous blocks is less than fissurized porous blocks. Addition, 'dipole moment', which is an 'energy' of the flow, mass of the fluid and front position of groundwater flow in fissurized porous blocks and cracks are also compared here.

Chapter 5: Summary and conclusion A summary of problems, input and output parameters are showed here to get an overview of all computational. A conclusion is also obtained from this studying.

2 Flow in homogeneous porous media

2.1 Model problem

The problem of the model mainly indicates a water level of saturated part for unsteady flow. A groundwater flow through a porous media supported by impermeable horizontal bottom and on the side by a vertical plane. The property of problem is groundwater flow in a river bank or channel bank after a short flood or after the breakthrough of a dam separating a channel or river from a reservoir of liquid waste. Dimensions of the flow are in positive x-direction along the bottom with origin $x = 0$ at the vertical plane and in y-direction as a height $y = h(x, t)$ (figure 2). At negative x-direction $x < 0$, a water reservoir is located. The horizontal extent of the stratum is considered to be semi-infinite: $0 \leq x < \infty$. Thus, the flow will never reach at the second boundary at ∞ and the front position will be discussed to see how far it moves into porous medium.

At time $t = -\tau$, the fluid level at $x = 0$ begins to increase rapidly to maximum height h_0 and decrease to initial distribution when $t = 0$. The boundary condition takes the form

$$h(0, t) = h_0 f(\theta), \qquad \theta = t/\tau. \tag{1}$$

The h_0 is a constant with the dimension of height, τ is a dimension of time. The $f(\theta)$ is a dimensionless function of its dimensionless argument, and is zero for $\theta = -1$ and $\theta < 0$, and nonnegative at $-1 < \theta < 0$. The function $f(\theta)$ was assumed to have a piecewise linear shape [1] that is defined in figures 8, 19 :

$$f(\theta) = \frac{\theta + 1}{\theta_* + 1}, \qquad -1 < \theta < \theta_* < 0; \tag{2}$$

$$f(\theta) = \frac{\theta}{\theta_*}, \qquad \theta_* < \theta < 0; \tag{3}$$

where θ_* a constant dimensionless time that function $f(\theta)$ is maximum.

Initially, the porous media is assumed to be empty. The initial condition is in the form

$$h(x, -\tau) \equiv 0, \qquad 0 \leq x < \infty. \tag{4}$$

In fact, the interval τ is a very short time. The groundwater flow happens as a very intense pulse at the boundary. In large times, $t = T \gg \tau$, i.e. $\theta \gg 1$ and $f(\theta)$ is not needed. The flow is considered gently sloping at

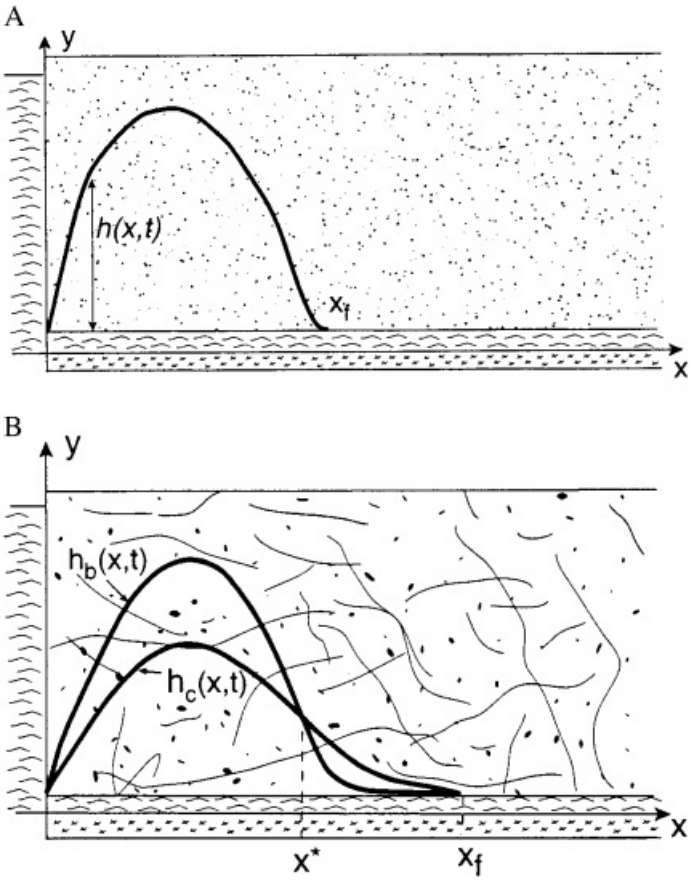

Figure 2: Groundwater dome extension in porous medium (A) and in fissurized porous medium (B) [1]. The h_B and h_C are the water levels in porous blocks and cracks.

large times. The water height is described by the Boussinesq equation (see refs. [2] [6] [7] [4]):

$$\frac{\partial h}{\partial t} = \kappa \frac{\partial^2 h^2}{\partial x^2}, \tag{5}$$

where the coefficient $\kappa = \frac{\rho g k}{2m\mu}$ is assumed a constant for a homogeneous porous medium, with μ the dynamic viscosity of the fluid, ρ the fluid density, k the permeability of porous medium and m its porosity. The initial-boundary values of the problem are:

$$\begin{aligned} h(x,0) &= h_i(x), \qquad 0 < x < \infty; \\ h(0,t) &= h(\infty,t) = 0, \qquad t > 0. \end{aligned}$$

2.2 Derive the Boussinesq equation

2.2.1 The physical model: Darcy's law

Fluid can flow through a porous media because a material has a porosity like sand is an example. The porosity is usually 40% in sandstone, while oil sands are in a range 10-20%. The flow is linearly driven by an applied pressure gradient and an inversely proportional to the viscosity. This is known as Darcy's law and was determined experimentally by Henry Darcy in 1856. The volumetric flow rate per unit area for a one-dimensional geometry is in the form:

$$Q = -\frac{kA}{\mu}\frac{dp}{dx}. \tag{6}$$

The permeability k is the resistance of the porous media. A practical unit for permeability is the darcy (D), or more commonly the millidarcy (mD) ($1darcy = 10^{-12}m^2$) [8]. For larger k, the smaller pressure gradient is needed to drive a given flow. For a homogeneous material, cracks here are considered very small fraction of this area. The greater pressure gradient increases the discharge rate per unit area, u. The discharge or the flux is referred as Darcy velocity, but it is not an actual velocity of the fluid [9]. This velocity is the average velocity per unit area. The discharge is in the form:

$$u = -\frac{k}{\mu}\frac{dp}{dx}. \tag{7}$$

In confined aquifer with a horizontal upper and lower boundary, the fluid is considered as an one-dimensional flow. That means the whole flow have an average velocity, density and other properties over a cross-section. The flow may be driven by an applied pressure gradient or the prescribed motion of the one of the cross-sections or maybe both [9]. Forces act on a layer of the fluid need to be balance to get a uniform flow as a single streamtube bounded by two streamlines the upper and lower boundaries (figure 3, (a)). The fluid moves with velocity u in the x-direction on the upper boundary with thickness h and the lower boundary is motionless. A uniform flow has a hydraulic head to balance the forces on the layer and the pressure drop in horizontal length. This head is the height of the fluid required to hydrostatically provide the applied pressure difference, $H \equiv \frac{p_1 - p_0}{\rho g}$ [9]. The horizontal velocity $u = u(y)$ varies only with the vertical coordinate in figure 3, (b). The hydraulic head of the flow in horizontal direction depends on x-direction, $h(x)$, a hydrostatic pressure distribution in the form

$$\frac{dp}{dx} = \rho g \frac{dh}{dx}. \tag{8}$$

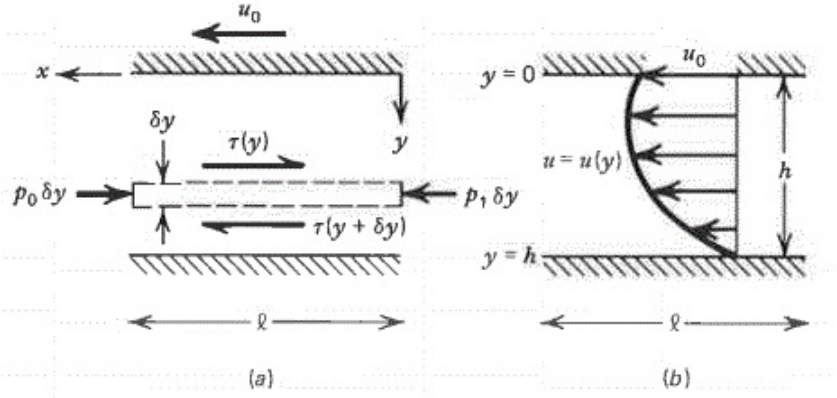

Figure 3: The force balance on a layer of fluid with an applied pressure gradient (a) and a profile of velocity (b) [9].

The Darcy velocity in the groundwater flow now can be in the form

$$u = -\frac{k\rho g}{\mu}\frac{dh}{dx}. \tag{9}$$

In unconfined aquifer, the water height is the height of the saturated-water region from a impermeable horizontal lower boundary to a phreatic surface as the upper boundary. A groundwater flow in unconfined aquifer is usually a two-dimensional flow with equipotential surfaces $\phi(x, y)$. The hydraulic head can not be used here. We need to assume the flow as an one-dimensional flow by using Dupuit approximation (figure 4). The phreatic surface in the Dupuit approximation is assumed as a parabola. The approximation is based from the results of the observation that in most groundwater flow, the slope of the phreatic surface is very small $dh/dx \ll 1$ [9]. At every point P along the phreatic surface, the specific discharge is given by the Darcy's law:

$$u_s = -\frac{k\rho g}{\mu}\frac{d\phi}{ds} = -\frac{k\rho g}{\mu}\frac{dy}{ds} = -\frac{k\rho g}{\mu} sin\theta. \tag{10}$$

As θ (slope) is very small, Dupuit suggested that $sin\theta = dy/ds = dh/ds$ can be replaced by $tan\theta = dh/dx$ [7]. The assumption of a gently sloping flow in Dupuit approximation is equivalent to assuming that vertical cross-sections are equipotential surfaces on which $h = \phi = constant$ and the flow essentially horizontal [7]. Thus, the Dupuit approximations lead to the specific discharge expressed by:

$$u_x = -\frac{k\rho g}{\mu}\frac{dh}{dx}. \tag{11}$$

The total rate of fluid flow is

$$Q_x = u_x h(x) = -\frac{k\rho g}{\mu} h \frac{dh}{dx}. \tag{12}$$

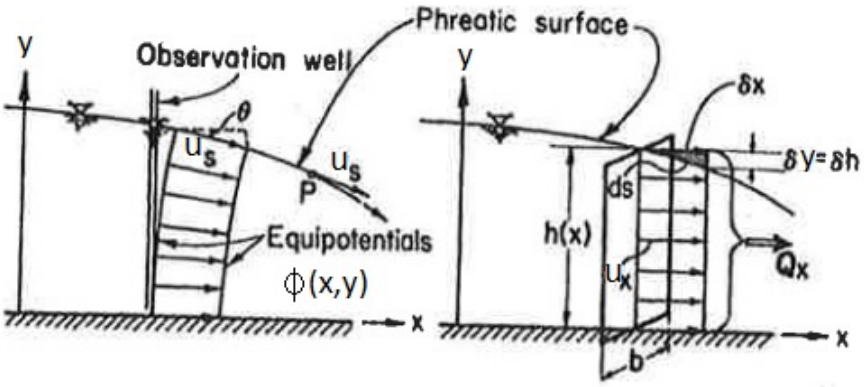

Figure 4: The Dupuit approximation [7].

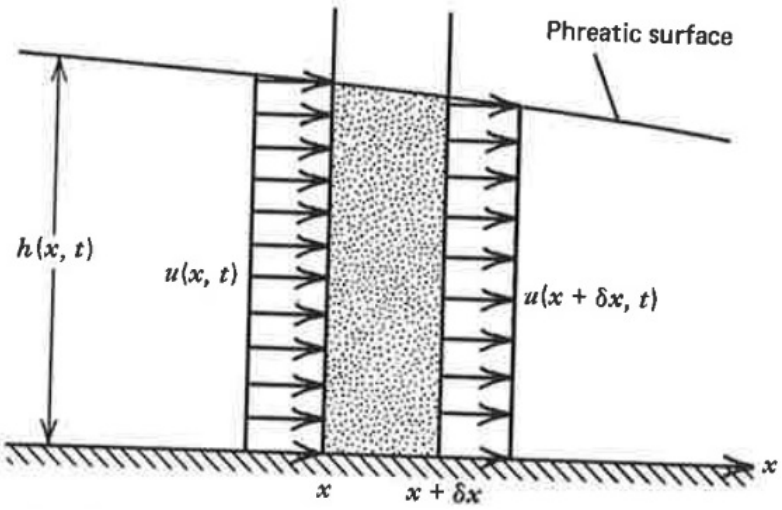

Figure 5: Conservation of mass of fluid through an element of an unconfined aquifer [9].

2.2.2 Unsteady flow

For unsteady flow, a flow rate through the aquifer varies with the time t. We assume the validity of Dupuit approximation and consider one-dimensional flow through an element of the unconfined aquifer from x to $x+\delta x$ (figure 5). The fluid is assumed incompressible (density is a constant). Conservation of mass of the fluid is needed.

The net rate of outflow through the element is

$$u(x+\delta x,t)h(x+\delta x,t) - u(x,t)h(x,t) \approx \frac{\partial}{\partial x}(uh)\delta x. \tag{13}$$

The height of the free surface changes because the inflow is not equal to the outflow. The change in the volume of the fluid in the element is

$$\phi[h(t+\delta t,x) - h(t,x)] \approx \phi\frac{\partial h}{\partial t}\delta x\delta t, \tag{14}$$

where ϕ the porosity in the matrix that the fluid fills it.

Conservation of mass of fluid needs that the net outflow of the element in time δt equals the decrease in fluid volume in the element so we get

$$\phi\frac{\partial h}{\partial t} + \frac{\partial}{\partial x}(uh) = 0. \tag{15}$$

Substitution of the Darcy velocity from equation 9 yields

$$\frac{\partial h}{\partial t} = \frac{k\rho g}{\mu\phi}\frac{\partial}{\partial x}(h\frac{\partial h}{\partial x}). \tag{16}$$

$$\frac{\partial h}{\partial t} = \frac{k\rho g}{2\mu\phi}\frac{\partial^2 h^2}{\partial x^2}. \tag{17}$$

This is the nonlinear diffusion equation is referred to as the Boussinesq equation [9].

2.3 Input parameters

A porous medium consists of a matrix and pores, which the fluid can flow through. The distribution of pores are usually irregular and different at each point. It is very difficult to describe a mathematical model for a porous medium. Properties such as velocity, porosity, density, etc., will be defined over a representative elementary volume (REV) to get average values [7]. Both matrix and pores are contained in the REV, which is determined large enough such that the volume average is representative for the centroid [10].

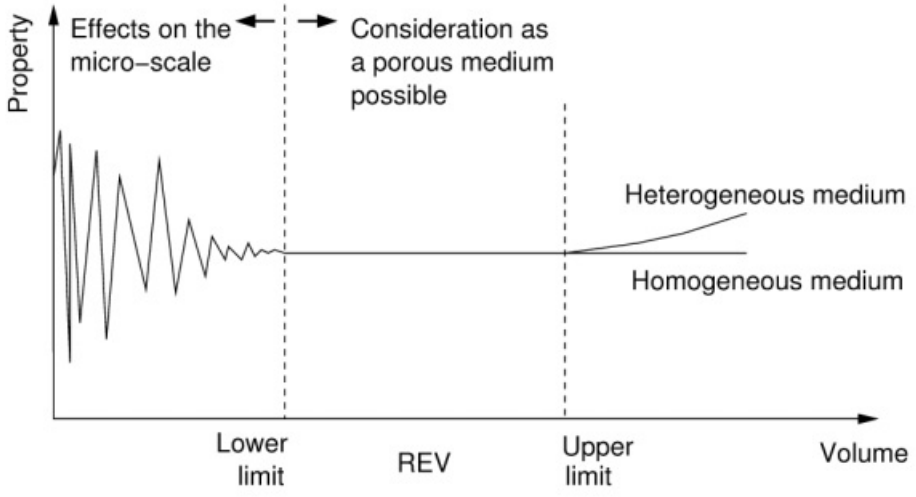

Figure 6: The scale of the representative elementary volume [10].

There are several important properties of the matrix and fluid that must be defined. Naturally, all the properties are functions depending on the pressure and the temperature.

The density of the fluid, ρ, is the mass over volume, and has units kg/m^3.

Viscosity is a property of the fluid and measures the resistance to flow. For large viscosity, the fluid is a thicker liquid. In practice, we use the dynamic viscosity and has units $kg/(m \cdot s) = Pa \cdot s = 10P(poise)$. There are density and viscosity of some common fluids in table 1 [10].

Gravitational acceleration, g, indicates the intensity of a gravitational field (m/s^2). At the surface of the earth, the g is about $9.8m/s^2$ [11].

Material	$\rho[kg/m^3]$	$\mu[10^3 Pa \cdot s]$
Air	1.205	0.02
Propane	1.882	0.11
Water	998	1.002

Table 1: Typical density ρ, and viscosity μ for a few common substances at atmospheric pressure and $20°C$.

The matrix properties are porosity m and permeability k of some common materials in the figure 7.

Material	Porosity [%]	Permeability [mD]
Brick	12–34	5–220
Granite	0.0005–1	500–2000
Limestone (dolomite)	4–10	2–45
Limestone (fine)	25–32	20–200
Sand	37–50	20000–180,000
Sandstone	8–38	0.5–3000
Shale	0.5–5	0–100
Soil	43–54	300–14,000

Figure 7: The porosity and permeability of some materials [10].

2.4 Numerical modeling for homogeneous porous medium

2.4.1 Discrete scheme of the model

The Boussinesq equation 17 that we derive above is a nonlinear equation. The parameters are dependent on the pressure. To solve this nonlinear problem is very difficult to use the Fourier method. The model is derived using a finite difference approximation of the initial-boundary values problem. The two-point boundary here is one from origin and one from infinite because the porous medium is assumed to extend very large and the front will never reach the second boundary. The way to derive the scheme is that the derivatives are replaced by finite differences by approximation for both the space and time derivatives.

Consider a discretization of the spatial domain $x \in [0, L]$ into $N+1$ cells. This gives the grid points $\{x_i\}_{i=1}^{N+1}$, where x_i is the center of the cell $I_i = [x_{i-1/2}, x_{i+1/2}]$. The length of each cell is $\triangle x = x_{i+1/2} - x_{i-1/2}$. All cells are same of the length.

A discretization of time is also considered of the time interval $t \in [0, T]$ into $Ntime$ steps with the same length, where T the total time length. The time steps is represented by time $\{t^k\}_{k=1}^{Ntime}$, where each time step has a length $\triangle t = t^{k+1} - t^k$.

A discrete scheme of the problem 5 with an explicit discretization in time then takes the following form

$$\frac{h_i^{n+1} - h_i^n}{\triangle t} = \kappa \frac{(\partial_x h^2)_{i+1/2}^n - (\partial_x h^2)_{i-1/2}^n}{\triangle x}, \qquad i = 1, ..., N+1, \tag{18}$$

where $(\partial_x h^2)_{i+1/2}^n \approx (\partial_x h^2)(x_{i+1/2}, t)$ for $t \in [t^k, t^{k+1}]$. A discrete of $\partial_x h^2$ at the interior part of the domain is considered

$$(\partial_x h^2)_{i+1/2}^n = \frac{(h^2)_{i+1}^n - (h^2)_i^n}{\triangle x}, \qquad i = 2, ..., N. \tag{19}$$

The numerical scheme of the interior part continues with the approximation

$$\frac{h_i^{n+1} - h_i^n}{\triangle t} = \kappa \frac{(h^2)_{i+1}^n - 2(h^2)_i^n + (h^2)_{i-1}^n}{(\triangle x)^2}. \tag{20}$$

This corresponds to

$$h_i^{n+1} = h_i^n + s[(h^2)_{i+1}^n - 2(h^2)_i^n + (h^2)_{i-1}^n], \qquad s = \kappa \frac{\triangle t}{(\triangle x)^2}. \tag{21}$$

The numerical model is solved by an explicit method, where different equations are algebraic equations. The differential operators are replaced

by algebraic approximation. This means explicit difference equations have the problem with the stability. The parameter, $s = \frac{\triangle t}{(\triangle x)^2}$, should be less than 0.5 to ensure stability for the discrete scheme [12]. This stability parameter will be investigated for such methods restrictions on time steps length and the space length to get the stabilized scheme.

The first cell and the last cell, the boundary conditions are employed which give the following value

$$h(1,k) = h(N+1,k) = 0. \tag{22}$$

The initial state is also followed by the scheme

$$h_i^1 = h_i^0 + s[(h^2)_{i+1}^0 - 2(h^2)_i^0 + (h^2)_{i-1}^0], \tag{23}$$

where $h(:, t = 0)$ the initial condition at large times.

The discrete scheme 21 is also an approximation in a short interval time $t = \tau \in [-1, 0]$ at the boundary $x = 0$. The water distribution at the initial $t = 0$ for large times case is found by simulating this first. The initial and boundary conditions of this initial problem are the following by

$$\begin{aligned} h(1,k) &= f(k), \qquad k < 1/\triangle t + 1, \\ h(1,k) &= 0, \qquad k \geq 1/\triangle t + 1, \\ h(N+1,k) &= 0, \\ h(i,1) &= 0. \end{aligned}$$

The dimensionless function $f(\theta)$ is defined clearly before the initial problem can be solved numerically. The procedure of the numerical solution is given in the following section.

2.4.2 Numerical solution

The model considers a length of porous media $L = 100$ with $N = 500$ cells with the length $\triangle x = \frac{L}{N} = \frac{100}{500} = 0.20$. The total time is $T = 2000$ and a short time interval $\tau = 1.0$ is considered at the boundary. The purpose of the large total time and the large length of the porous blocks is that the flow can not reach the boundary at infinity, so the front of groundwater mound can be investigated in different times. With the time steps is $Ntime = 200000$, the length time steps is $\triangle t = T/Ntime = 0.01$. Because of the "frozen" coefficient $\kappa = 0.20$, the numerical model is observed by different time steps to get the stability condition $s = \kappa \frac{\triangle t}{(\triangle x)^2} = 0.20 \frac{0.01}{0.20^2} = 0.05$.

At first, the function $f(\theta)$ is defined with the maximum water level $h_0 = 10.00$ and $\theta_* = -0.80$, so the profile of the water level at the boundary takes as the figure 8. The maximum water level h_0 reaches at θ_* and decreases to the initial distribution, which is assumed to be zero at time $t = -\tau$ and $t = 0$.

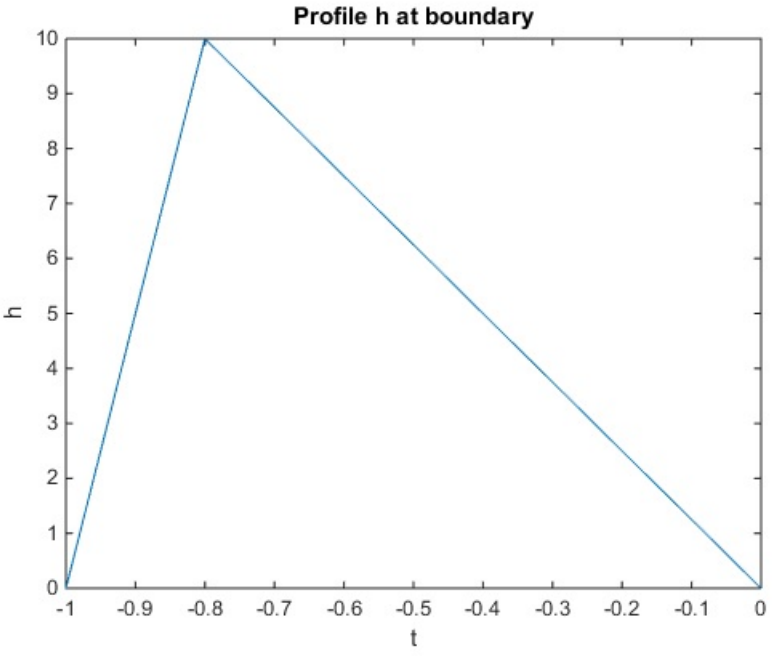

Figure 8: Profile of the water height at the boundary from $t = -1.00$ to $t = 0$ with $\theta_* = -0.80$.

Secondly, the initial state is solved by numerical scheme 23 with two-point boundary: one at the origin $x = 0$ and one at infinite, which the total length is considered very large $L = 100.00$. The left boundary is defined

from the profile water height at the boundary above. The initial distribution at $t = -\tau$ is zero. The result of this scheme is the water height of groundwater flow at time $t = 0$, i.e after a small time $\tau = 1.00$, or the initial distribution of the discrete model. The figure 9 shows that the groundwater flow with an intense pulse at the boundary now becomes the initial distribution in the porous blocks. This happens in a very short time after a breakthrough of the dam. The water height is less than half of the maximum of the pulse and begin to extend further in the porous medium.

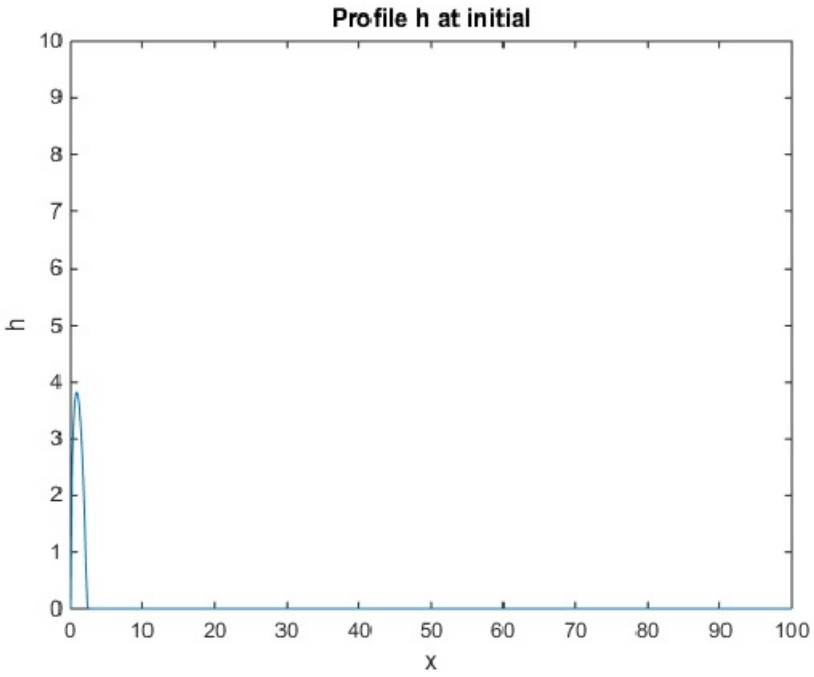

Figure 9: Profile of the initial height distribution $t = 0$.

The numerical model 21 is simulated to get the water height after $t = 0$. A results of the numerical solution is plotted in figure 10. All of the water levels are less than the initial distribution and the positions of the front of groundwater flow go further at large times. The mass of the groundwater mound looks the same in smaller times ($t < 10.00$), but it is very difficult to see a constant in large times from $t = 10.00$. The dipole moment at $t = 0$ is also obtained a constant, $Q = 6.67$, by following equation

$$Q = \sum_{i=1}^{N+1} x(i)h_i(i)\triangle x. \tag{24}$$

The dipole moment indicates an energy that groundwater flow needs to move through the porous medium. This energy is at the maximum initially and is not changed with time that the numerical solution has a stability estimate [12]. This will be proofed in the next section.

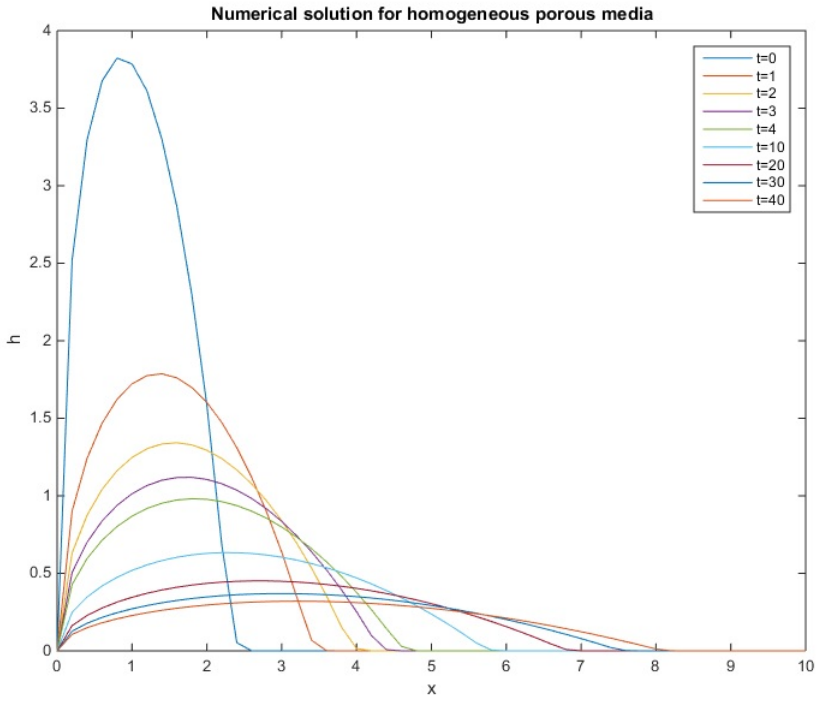

Figure 10: The water height of the groundwater flow using numerically.

2.5 Analytical analysis of the model

2.5.1 The analytical solution from references

Before the model can be calculated by analytically, the conditions need to be clearly. The groundwater flow, which happens from a very intense pulse in the model problem continues with a large times. At the boundary, the function $f(\theta)$ is not needed. Thus, the boundary conditions are in the forms

$$h(0,t) = 0,$$
$$h(\infty,t) = 0.$$

This is why the fluid mound extends further into the porous medium at every time $t > 0$ [13]. After a short time τ, a porous medium has the initial water height distribution $h_i(x)$ at $t = 0$. The fluid level at the boundary is zero for $t > 0$. Therefore, the initial condition takes form [13]

$$h(x,0) = h_i(x), \qquad 0 < x < \infty. \tag{25}$$

The model with these conditions was solved by Barenblatt and Zel'dovich in 1957 [14]. The conditions indicate that the water level h vanishes at origin $x = 0$ and at the front of the groundwater mount $x = x_f(t)$ [15]. Dipole moment Q was also defined from [14] by the following equation

$$Q(t) = \int_0^\infty xh(x,t)dx. \tag{26}$$

The dipole moment Q of the initial water height distribution at $t = 0$ is defined by

$$Q(t=0) = \int_0^\infty xh(x,0)dx = \int_0^\infty xh_i(x)dx. \tag{27}$$

We integral the dipole moment with time

$$\frac{d}{dt}Q(t) = \frac{d}{dt}\int_0^\infty xh(x,t)dx = \int_0^\infty x\kappa\frac{\partial^2 h^2}{\partial x^2} = \kappa[x(\frac{h}{2}\frac{\partial h}{\partial x}) - h]_0^\infty = \kappa h(0,t). \tag{28}$$

Since the fluid stops to drain out at the boundary $x = 0$, so the volume per unit width of the fluid is conserved. Thus, the dipole moment is a constant and equals to $Q(t = 0)$ at arbitrary time $t > 0$.

$$\frac{d}{dt}Q(t) = \frac{d}{dt}\int_0^\infty xh(x,t)dx = 0. \tag{29}$$

At every motion of the fluid, the constancy of the dipole moment indicates that the model can find a self-similar solution for the motion [15].

Here, the similar scalings are used, which is developed by Barenblatt and Zeldovich in 1957 [14] based on equations were 5 and 26. The similarity arguments indicate that [15]

$$h \sim \frac{x^2}{\kappa t} \tag{30}$$

$$Q \sim x^2 h \tag{31}$$

The height h is eliminated so that the scale of the length of the flow yields

$$x \sim (\kappa Q t)^{\frac{1}{4}}. \tag{32}$$

Following these scalings, we get the self-similar solution in the form

$$h = (\frac{Q}{\kappa t})^{\frac{1}{4}} \phi(\gamma), \qquad \gamma = \frac{x}{(\kappa Q t)}^{\frac{1}{4}}. \tag{33}$$

The front of the groundwater flow here is $x_f = \gamma_0 (\kappa Q t)^{\frac{1}{4}}$ [14]. The function $\phi(\gamma)$ is obtained by substituting 33 into equations 5 and 26, yields an ordinary differential equation for $\phi(\gamma)$ [14] and yields

$$\frac{d^2\phi^2}{d\gamma^2} + \frac{\gamma}{2}\frac{d\phi}{d\gamma} + \frac{\phi}{2} = 0, \tag{34}$$

$$\int_0^\infty \gamma\phi(\gamma) d\gamma = 1. \tag{35}$$

The boundary conditions now become

$$\phi(0) = 0, \tag{36}$$

$$\phi(\gamma_0) = 0. \tag{37}$$

Multiplying the equation 34 by γ, integrating by parts, and applying the first boundary condition 36 yields [15]

$$\gamma\frac{d\phi}{d\gamma} - \frac{\phi}{2} + \frac{1}{4}\gamma^2 = 0. \tag{38}$$

This is a first-order differential equation in ϕ. The equation is continued with a further integration and by applying the second condition 37, the function ϕ is obtained

$$\phi(\gamma) = \frac{\gamma_0^2}{12}(\frac{\gamma}{\gamma_0})^{\frac{1}{2}}[1 - (\frac{\gamma}{\gamma_0})^{\frac{3}{2}}], \qquad 0 \le \gamma \le \gamma_0;$$

$$\phi(\gamma) = 0, \qquad \gamma \ge \gamma_0.$$

Substituting the solution of ϕ into the equation 35, it gives $\gamma_0 = 2\sqrt[4]{5}$. Let introduce the variable $\zeta = \frac{\gamma}{\gamma_0}$, so the function $\phi(\gamma)$ is now in the form

$$\phi(\zeta) = \frac{\sqrt{5}}{3}\zeta^{\frac{1}{2}}[1 - \zeta^{\frac{3}{2}}], \qquad 0 \leq \zeta \leq 1; \tag{39}$$

$$\phi(\zeta) = 0, \qquad \zeta \geq 1. \tag{40}$$

2.5.2 The exact analytical solution

The continuous problem of the Boussinesq equation 5 for a homogenous porous media is plotted by using the exact analytical solution 41.

$$h = (\frac{Q}{\kappa t})^{\frac{1}{4}}\phi(\zeta), \qquad \zeta = \frac{x}{x_f}. \tag{41}$$

The position of the front equals to

$$x_f(t) = 2(5\kappa Q t)^{\frac{1}{4}}.$$

Function $\phi(\zeta)$ is obtained in equations 39, 40. Dipole moment is $Q = 6.67$, which is defined from the numerical solution. The results in figure 11 show the exact solution of the model. The maximum water level is the initial distribution and decreases when time is larger. The front of the groundwater flow does not reach at $h = 0$ seen clearly at small times. The water level reaches $h = 0$ when function $\phi(\zeta)$ is zero at $\zeta = \frac{x}{x_f} \geq 1$. But $\frac{x}{x_f}$ does not exact 1 and ϕ is equivalent to zero, so the water level is just near zero at the front of flow or $h \equiv 0$. Thus, the exact analytical solution is obtained (figure 11) from the following equations

$$h = (\frac{Q}{\kappa t})^{\frac{1}{4}}\phi(\zeta), \qquad \zeta = \frac{x}{x_f},$$

$$\phi(\zeta) = \frac{\sqrt{5}}{3}\zeta^{\frac{1}{2}}[1 - \zeta^{\frac{3}{2}}], \qquad 0 \leq \zeta \leq 1;$$

$$h \equiv 0, \qquad \zeta \geq 1.$$

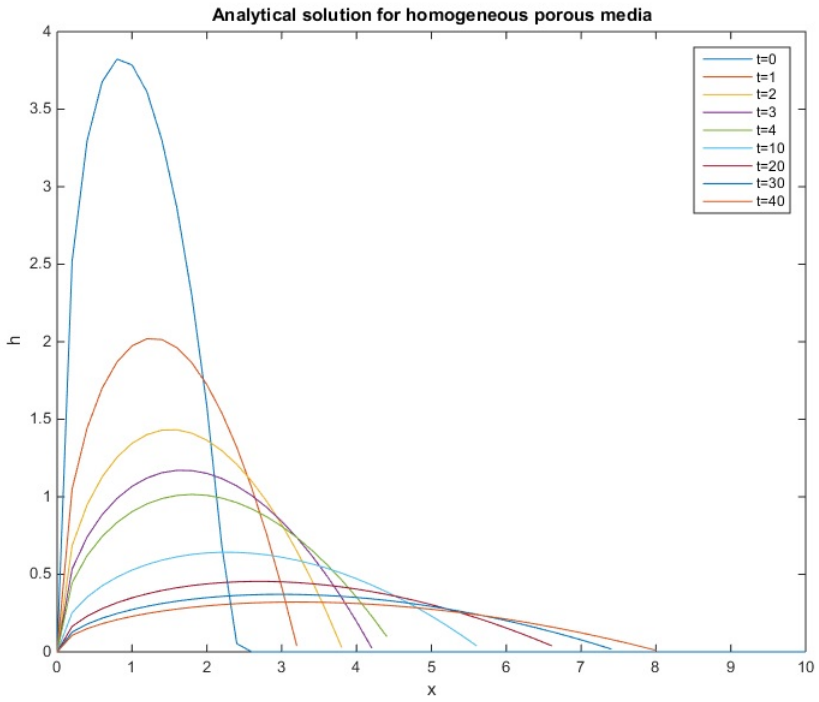

Figure 11: The water height of the groundwater flow using analytically. The water height at the initial $t = 0$ is computed by numerically.

2.6 More investigation about solutions

Firstly, the maximum height h_0 affects on the smooth of the both solution. The solutions are solved with the same length $x \in [0, 100]$ and $T \in [0, 2000]$, so the stability parameter keeps the same $s = 0.05$. The model is only change the $h_0 = 1.00$. From the figures 12 and 13, changing the maximum water level , several oscillations appear in both solutions.

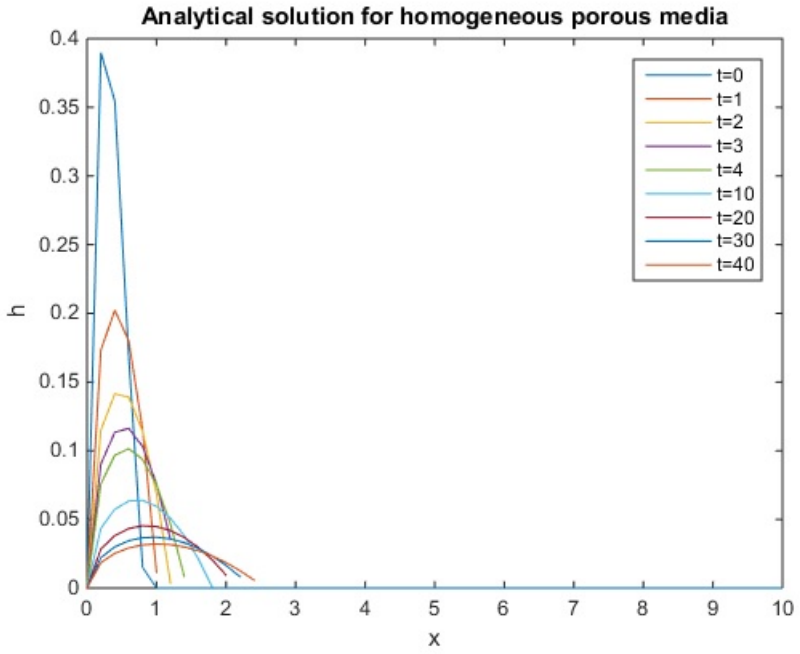

Figure 12: The analytical solution with $h_0 = 1.00$.

Secondly, the stability parameter is smaller in comparison with the condition $s \leq 1/2$, but how the maximum its can be to get good results. The reason is the large time and space are used here. If changing the parameter $s = 0.10$, the number of cells is also changed to $N = 5000$, and the time steps is the same. The memory of the observed computer can not handle such large cells.

The time steps now is changed to $Ntime = 100000$ and the length of time steps is $\triangle t = 0.02$. The stability parameter $s = 0.2\frac{0.02}{0.2^2} = 0.10$. The grids points $x(i)$ become a nonrepresentable number (NaN) and the process stops to run the model.

The stability parameter is changed to $s = 0.06$, that means the time steps changes to $Ntime = 166667$ and the length is $\triangle t = T/Ntime = 2000/166667 = 0.01$. The grids points $x(i)$ still become a nonrepresentable

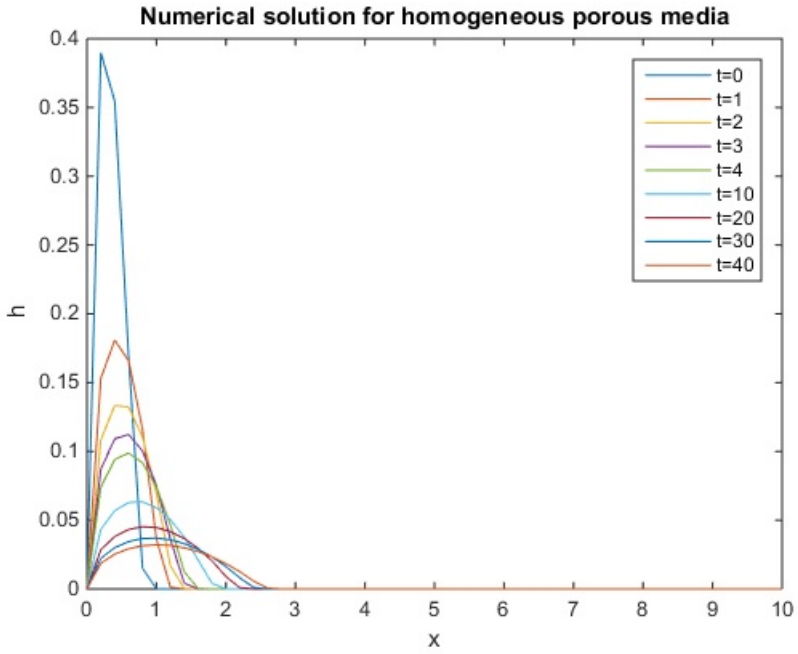

Figure 13: The numerical solution with $h_0 = 1.00$.

number (NaN). Therefore, the stability parameter should be less than 0.05 to simulate the model.

2.7 Comparison the results

The model problem for homogeneous porous medium has both a continuous solution and a discrete solution from explicit method. The groundwater flow at $t = 0$ between the solutions has to be equal because they are both simulated during a short time $-1 \leq t \leq 0$. From the figures 10 and 11, the front $x_f(t)$ of the groundwater flow are show in the table 2. The front positions of the numerically go faster than the analytically at time $t < 10.00$.

Time	Analysis	Numeric
t=0	2.60	2.60
t=1.00	3.23	3.60
t=2.00	3.90	4.20
t=3.00	4.24	4.60
t=4.00	4.60	4.80

Table 2: The front $x_f(t)$ of the groundwater flow.

Results from the analytical and numerical solutions above are plotted together in the same figure for comparison. The figure 14 represents the results of the water levels at time, which is less than $t = 10.00$. The analysis solutions (blue circle line) are higher than the numerical solutions (red line). At time is equal $t = 10.00$, the two lines is almost match together in figure 15. When times are larger than $t = 10.00$, both solutions are equal and lie in the same lines.

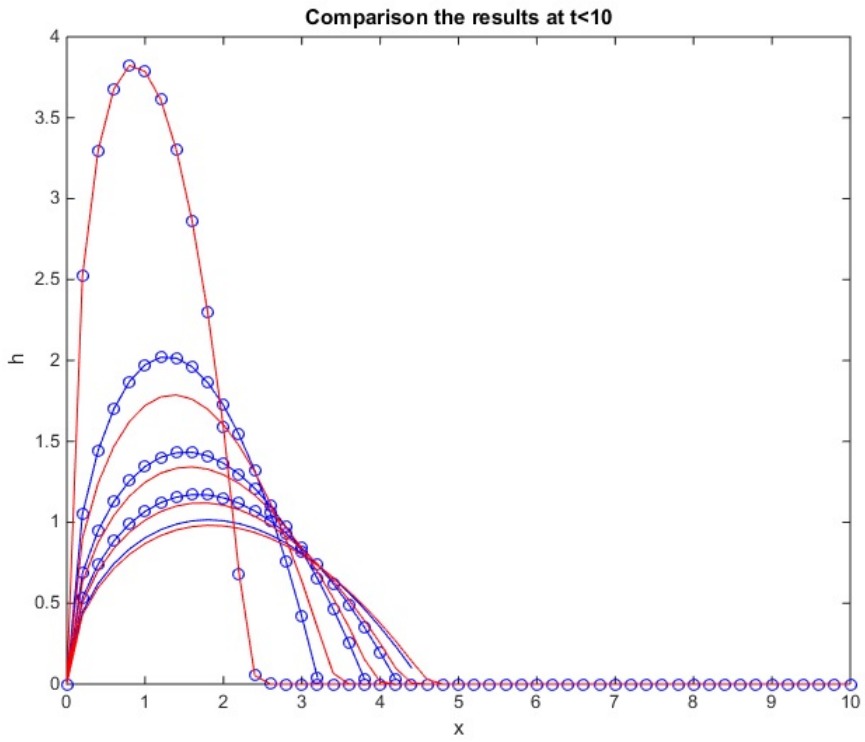

Figure 14: The water levels from analysis solution (blue circle line) and numerical solution (red line) at times less than $t = 10.00$.

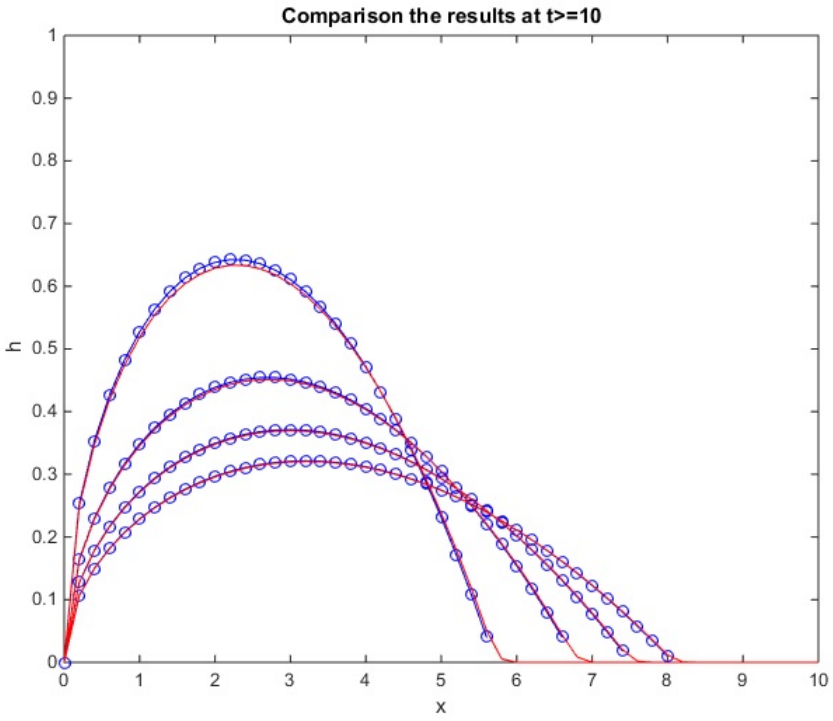

Figure 15: The water levels from analysis solution (blue circle line)and numerical solution (red line) with times from $t = 10.0$.

3 Flow in stratified heterogeneous porous media

In this section, a stratified heterogeneous porous medium is considered (κ is not a constant). A fluid flows through two porous mediums separated by a slightly permeable intervening layer in figure 16 [4]. This problem is known as flow in stratified porous medium or in a 'double' porous medium in which the majority of the permeability is provided by fractures while the majority of storage is provided by porous blocks [3]. A double-porosity medium can be in a multilayer system (figure 16) or in a natural fracture system (a fissurized reservoir in figure 17).

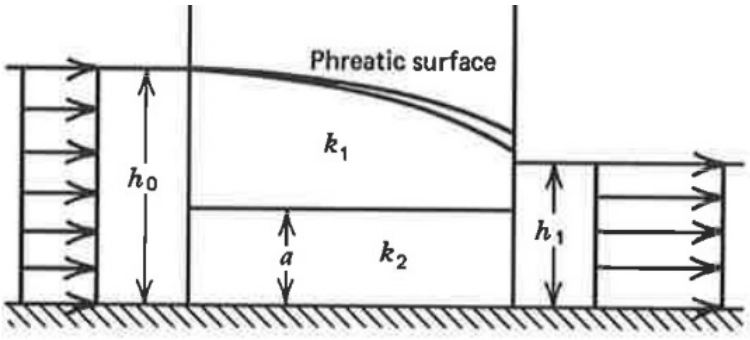

Figure 16: An example of a fluid flow in a stratified heterogeneous porous medium [9]. A flow goes through two porous medium with permeabilities k_1, k_2.

The reason for studying fractured media is that a number of large oil fields are confined to fractured reservoirs [4]. There is widely a uniform rock was deformed to fractured rock in nature. These fractures caused by tectonic stresses, or a chemical process when water dissolved the rock matrix [4]. The degree of fractures may be different in rocks. When we look at a large scale, the fracture is assumed that it does not exist. This homogeneous rock is easier to calculate a fluid flow through a natural rock. A lot of results of theoretical and laboratory investigation of unsteady flow with data for strata under natural conditions obtain that calculating flow through a homogeneous porous media is not enough [5].

In this studying, a porous media with a system of fissures, which are small natural fractures is considered regular to some extent (on the right of figure 17). An exchange flow, which moves from porous blocks and cracks, is assumed as a steady flow. A 'double-porosity' model in fissured rocks was described by Barenblatt & Zheltov in 1960 [5] and by Barenblatt et al. in

1990 [4]. By combining with the Boussinesq equation, a system equations for water level of fissurized porous blocks and system cracks are described and simulated from computational experiment by numerically. The results are compared with the results in an ordinary porous medium that show how the fissures influence the flow in a heterogeneous porous media.

3.1 Continuum approach

A fractured rocks usually consists of a system of irregular shape and arrangement of porous blocks and separated by fissures. The data characteristics is taken from the cores are incomplete on fractures system. In the left figure 17, there represents two porous system in the naturally fractured rocks: a matrix blocks with high storage capacity and low permeability and a system of fracture with high permeability and low storage capacity. The flow between systems happens separately and an interporosity flow takes place between them. The interporosity flow is based on the theory of seepage that the solid matrix of a porous medium is impermeable and the fluid move within them [4]. The fractures here play the role of pores and the blocks play the role of grains in the right figure 17. An analysis of flow in porous blocks between a regular system of cracks is the flow with a continuum approach [4].

An applied of continuum approach is used for a complexity of naturally fractured networks. Some average characteristics (porosity, permeability, pressure, seepage velocity, etc.) of the flow and medium take over a scale which is large compared to the dimensions of the individual blocks [16]. The formulation of physical laws is based on these mean characteristics of a system of cracks in fractured rocks.

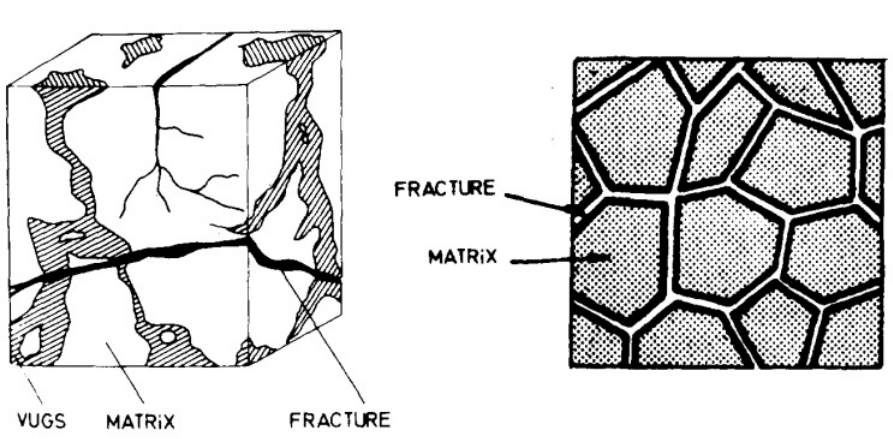

Figure 17: A continuum model approach from naturally fractured reservoir [10].

3.2 Fracture model

3.2.1 The exchange flow

The fracture geometry The specific characteristic of the fissures is that the crack can be viewed as a narrow gap, a length along the two parallel plates and a constant width of aperture, which is perpendicular to the length are two dimensions that are several orders of magnitude higher than the third (figure 18) [4]. The length of the cracks is much wider than pores and the volume of a system of cracks is a small part in comparison with pores [1]. The porous blocks are considered with dimensions H height, W width and L length [17] in figure 18. The fissure is also defined between the blocks as the fracture centre plane. The flow in fissures is assumed a laminar flow between two parallel impermeable blocks and follows the hydraulic Darcy velocity in equation 9 on the basic of two dimensional analysis of each fissure.

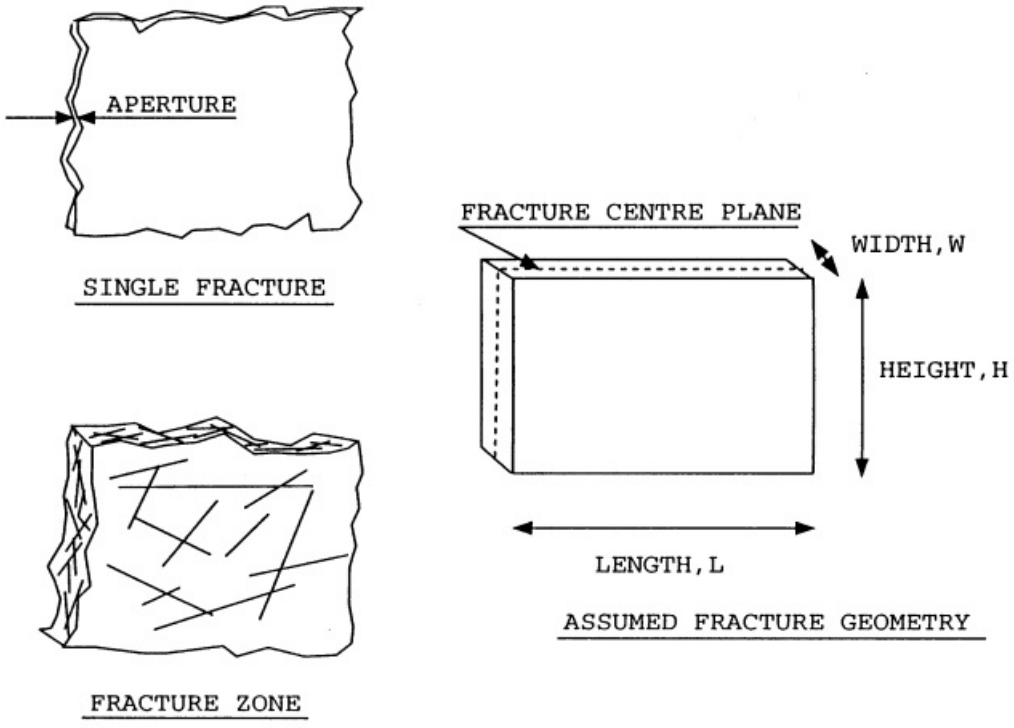

Figure 18: Fracture geometry [17].

The different flows in two porous system have separate water heights for blocks $h_B = h_B(x,t)$ and for cracks $h_C = h_C(x,t)$. At the boundary between the blocks and the system cracks, the process of transfer of fluid from

the blocks and the system cracks takes place under a smooth change of pressures: an initial pressure p_0 in the porous blocks and a pressure $p_1 < p_0$ when the groundwater flow breakthrough at the boundary. The pressure difference $p_0 - p_1$ takes place in the porous blocks with the length L and the system of cracks with the length of the reservoir $l \gg L$. Thus, the pressure drop of the porous blocks $(p_0 - p_1)/L$ is bigger than the pressure drop of the system cracks $(p_0 - p_1)/l$ and follows that the exchange flow happens between the porous blocks and system cracks [4]. This exchange flow will appear after a transient flow. To approach the continuum model, the transient flow is considered with a short time interval, τ, at the boundary. So, the exchange flow is assumed a quasi-steady flow from the initial distribution ($t \geq 0$) and independent of time explicit.

If we use the discrete fracture model, i.e., each fissure is modelled explicitly. In fact, the system of fissures here is a small part in the field and it is impossible to get the detail information about the field geometry and fractures characteristics. That is why we use the length of the reservoir to get the average parameters of the system cracks. These models are based on an approximation by only several fissures significance and the system are treated as non-homogeneous medium [10].

The exchange flow is derived from the total discharge q per unit width through a vertical cross-section of the porous blocks for steady state by following equation

$$q = u(x)h(x) = -\frac{k_B \rho g}{\mu} h \frac{dh}{dx}. \tag{42}$$

The mass conservation requires the total discharge q is constant; the same amount of fluid should cross each surface per unit time. Integrating between $x = 0$ and a distance of the length of the blocks $x = L$, which is large in comparison with the pore size d but small in comparison with the size of the reservoir l ($d \ll L \ll l$) [4] we obtained

$$\begin{aligned} qdx &= -\frac{k_B \rho g}{\mu} h dh \\ q \int_{x'=0}^{x=L} dx' &= -\frac{k_B \rho g}{\mu} \int_{h'=h_B}^{h_C} h' dh' \\ q &= -\frac{k_B \rho g}{\mu 2L} (h_B^2 - h_C^2). \end{aligned}$$

This equation is known as the Dupuit-Forchheimer discharge formula [7].

The exchange flow from the system fissures and the porous blocks is based on the equation above and has the following form

$$q = -\alpha (h_B^2 - h_C^2), \tag{43}$$

where $\alpha = \frac{k_B \rho g}{\mu 2L}$ is an exchange coefficient and is assumed to be constant.

3.2.2 Double-porosity model

Based on an applied continuum approach, a principle of mass conservation is used here to derived a continuity equation. The state of conservation of mass is:

change of mass + net outflow of a volume = change of mass due to sources/sinks [10].

In mathematical terms, the mass conservation yields

$$m\frac{\partial h}{\partial t} + \frac{\partial}{\partial x}(uh) = q. \tag{44}$$

Substituting the equations 7 and 43, the double-porosity model yields

$$m\frac{\partial h_B}{\partial t} = \kappa_B m\frac{\partial^2}{\partial x^2}h_B^2 - \alpha(h_B^2 - h_C^2), \tag{45}$$

$$m\epsilon\frac{\partial h_C}{\partial t} = \kappa_C m\epsilon\frac{\partial^2}{\partial x^2}h_C^2 + \alpha(h_B^2 - h_C^2), \tag{46}$$

where ϵ is the ratio of the cracks porosity, relative to a volume of cracks, to the porosity of the porous blocks. The coefficients κ_B and κ_C are the same form as the equation 5 of the Boussinesq equation

$$\kappa_B = \frac{\rho g k_B}{2m\mu},$$

$$\kappa_C = \frac{\rho g k_C}{2m\epsilon\mu},$$

where k_B the permeability of the porous blocks and k_C the permeability of the system of cracks. The ratio ϵ is very small, $\epsilon \ll 1$, so the $\kappa_B \ll \kappa_C$.

The initial and boundary conditions The conditions are the same as the model problem of a very intense pulse. At the boundary, the groundwater flow increases rapid to maximum level h_0 and decreases to initial distribution, which is assumed to zero, at a short time interval τ. The boundary condition is in the form

$$h_B(0,t) = h_C(0,t) = h_0 f(\frac{t}{\tau}). \tag{47}$$

The function $f(\theta) \equiv 0$ at $\theta > 0$, $f(-1) = f(0) = 0$ and $f(\theta) > 0$ at $-1 < \theta < 0$ [1]. The initial condition is assumed

$$h_B(x,-\tau) = h_C(x,-\tau) \equiv 0, \qquad 0 \le x < \infty. \tag{48}$$

From this condition, the dome extension has a finite speed and the boundary at infinity is added

$$h_B(\infty, t) = h_C(\infty, t) \equiv 0. \tag{49}$$

Dipole moment We consider the groundwater flow with $t \geq 0$. The purpose of this is that we obtain a constancy of the dipole moment and follows a conservation of mass of fluid. The models, which are based on the Boussinesq equation are validly to calculate the water level of the saturated-region in an unconfined aquifer through a fissurized porous medium. The equation 45, 46 are divided by porosity, m,

$$\frac{\partial h_B}{\partial t} = \kappa_B \frac{\partial^2}{\partial x^2} h_B^2 - \frac{\alpha}{m}(h_B^2 - h_C^2), \tag{50}$$

$$\epsilon \frac{\partial h_C}{\partial t} = \kappa_C \epsilon \frac{\partial^2}{\partial x^2} h_C^2 + \frac{\alpha}{m}(h_B^2 - h_C^2). \tag{51}$$

The dipole moment in the case of the system of equations 50-51 and together with the conditions 47, 48, 49 has an integral of the same dipole moment type [1]

$$Q(t=0) = \int_0^\infty x[h_B(x,t) + \epsilon h_C(x,t)]dx. \tag{52}$$

This integral is derived with d/dt, added the equations 50 and 51, multiplied with x and integrated from $x = 0$ to $x = \infty$. The second terms in the system equations 50-51 vanish because the exchange flow does not happen at the time that an intense pulse breakthrough a dam. So, we obtain

$$\begin{aligned}
\frac{d}{dt}Q(t) &= \frac{d}{dt}\int_0^\infty x h_B(x,t)dx + \frac{d}{dt}\int_0^\infty x\epsilon h_C(x,t)dx \\
&= \int_0^\infty x\kappa_B \frac{\partial^2}{\partial x^2} h_B^2 dx + \int_0^\infty x\kappa_C \frac{\partial^2}{\partial x^2} h_C^2 dx \\
&= \kappa_B[x(\frac{h_B}{2}\frac{\partial h_B}{\partial x}) - h_B]_0^\infty + \kappa_C[x(\frac{h_C}{2}\frac{\partial h_C}{\partial x}) - h_C]_0^\infty \\
&= \kappa_B h_B(0,t) + \kappa_C h_C(0,t).
\end{aligned}$$

When $t \geq 0$, the boundary and initial conditions yield

$$h_B(0,t) = h_C(0,t) = 0, \tag{53}$$

$$h_B(x,0) = h_{iB}(x), \tag{54}$$

$$h_C(x,0) = h_{iC}(x). \tag{55}$$

The groundwater flow stops to drain out at the boundaries. Thus, the dipole moment is a constant and equals the dipole moment at initial distribution.

$$\begin{aligned} Q(t) = Q(t=0) &= \int_0^\infty x[h_B(x,0) + \epsilon h_C(x,0)]dx, \\ &= \int_0^\infty x[h_{iB}(x) + \epsilon h_{iC}(x)]dx. \end{aligned}$$

3.3 Numerical experiment

3.3.1 Dimensionless variables

The system equation are simplified by introducing dimensionless variables.

Dimensionless time is $\theta = \frac{t}{\tau}$. Definition dimensionless time by $\frac{\partial}{\partial t} = \partial_t$ yields

$$\partial_t = \frac{\partial \theta}{\partial t}\partial_\theta = \frac{1}{\tau}\partial_\theta. \tag{56}$$

The water levels of the porous blocks and the system cracks are $H_B = \frac{h_B}{h_0}$ and $H_C = \frac{h_C}{h_0}$. Adding to the basic system equations, we calculate the dimensionless position and the dimensionless exchange coefficient. From the first equation for the porous blocks yields

$$\begin{aligned}
\frac{h_0}{\tau}\partial_\theta H_B &= \kappa_B h_0^2 \partial_{xx}^2 H_B^2 - \frac{\alpha h_0^2}{m}(H_B^2 - H_C^2), \\
\partial_\theta H_B &= \kappa_B h_0 \tau \partial_{xx}^2 H_B^2 - \frac{h_0 \tau \alpha}{m}(H_B^2 - H_C^2).
\end{aligned}$$

The second equation for the system cracks yields

$$\begin{aligned}
\frac{h_0}{\tau}\partial_\theta H_C &= \kappa_C h_0^2 \partial_{xx}^2 H_C^2 - \frac{\alpha h_0^2}{m\epsilon}(H_B^2 - H_C^2), \\
\partial_\theta H_C &= \kappa_C h_0 \tau \partial_{xx}^2 H_C^2 - \frac{h_0 \tau \alpha}{m\epsilon}(H_B^2 - H_C^2).
\end{aligned}$$

The dimensionless positions are differences in two equations because of the coefficients κ_B and κ_C.

$$\begin{aligned}
\partial_{\xi\xi}^2 &= \kappa_B h_0 \tau \partial_{xx}^2, \\
\partial_{\xi\xi}^2 &= \kappa_C h_0 \tau \partial_{xx}^2.
\end{aligned}$$

These correspond to

$$\begin{aligned}
\kappa_B \partial_{xx}^2 &= \frac{1}{h_0 \tau}\partial_{\xi\xi}^2, \\
\kappa_C \partial_{xx}^2 &= \frac{1}{h_0 \tau}\partial_{\xi\xi}^2.
\end{aligned}$$

Elimination the κ_C in the second equation above yields

$$\begin{aligned}
\frac{\kappa_B}{\kappa_C}\partial_{xx}^2 &= \frac{1}{\kappa_C \tau h_0}\partial_{\xi\xi}^2, \\
\partial_{xx}^2 &= \frac{1}{\kappa_C \tau h_0}\partial_{\xi\xi}^2.
\end{aligned}$$

So, the dimensionless position is in the form

$$\partial^2_{xx} = \frac{\partial \xi^2}{\partial x^2}\partial^2_{\xi\xi} = \frac{1}{\kappa_C \tau h_0}\partial^2_{\xi\xi},$$
$$\xi = \frac{x}{\sqrt{\kappa_C \tau h_0}}.$$

The exchange coefficient α now has a dimensionless form, β,

$$\beta = \frac{\alpha \tau h_0}{m}. \tag{57}$$

We can reduce the basic system of equations into a convenient dimensionless form:

$$\partial_\theta H_B = \frac{\kappa_B}{\kappa_C}\partial^2_{\xi\xi} H_B^2 - \beta(H_B^2 - H_C^2), \tag{58}$$
$$\partial_\theta H_C = \partial^2_{\xi\xi} H_C^2 + \frac{\beta}{\epsilon}(H_B^2 - H_C^2). \tag{59}$$

The boundary and initial conditions are also in the dimensionless form

$$H_B(0,\theta) = H_C(0,\theta) = f(\theta), \tag{60}$$
$$H_B(\xi,-1) = H_C(\xi,-1) \equiv 0, \tag{61}$$
$$H_B(\infty,\theta) = H_C(\infty,\theta) = 0. \tag{62}$$

The function $f(\theta)$ here is also the dimensionless function, $f(\theta) \equiv 0$ at $\theta \geq 0$. The system equations 58-59 are considered with semi-infinite $0 \leq \xi < \infty$ and time $\theta > -1$. The total dipole moment is also simplified in dimensionless form, M,

$$\int_0^\infty \sqrt{\kappa_C \tau h_0}\xi h_0 (H_B + \epsilon H_C)\sqrt{\kappa_C \tau h_0} d\xi = Q,$$
$$M = \frac{Q}{\kappa_C \tau h_0^2} = \int_0^\infty \xi (H_B + \epsilon H_C) d\xi.$$

3.3.2 Discrete schemes

A system of equations 58 and 59 is consider with the spatial domain $\xi \in [0, L]$ and $\theta \in [0, T]$. The $N + 1$ cells are also used in the fissures-porous blocks with the same length $\triangle\xi = \xi_{i+1/2} - \xi_{i-1/2}$. This gives the grid points $\{\xi_i\}_{i=1}^{N+1}$, where ξ_i is the center of the cell $I_i = [\xi_{i-1/2}, \xi_{i+1/2}]$. The time steps $Ntime$ and the length of each time step $\triangle\theta = \theta^{k+1} - \theta^k$ are considered the same as with the homogeneous porous medium case. The time steps is represented by time $\{t^k\}_{k=1}^{Ntime}$.

The solution of the system equations are approximated by the schemes

$$\frac{(H_B)_i^{n+1} - (H_B)_i^n}{\triangle\theta} = \frac{\kappa_B}{\kappa_C} \frac{(H_B^2)_{i+1}^n - 2(H_B^2)_i^n + (H_B^2)_{i-1}^n}{(\triangle\xi)^2} - \beta[(H_B^2)_i^n - (H_C^2)_i^n], \tag{63}$$

$$\frac{(H_C)_i^{n+1} - (H_C)_i^n}{\triangle\theta} = \frac{(H_C^2)_{i+1}^n - 2(H_C^2)_i^n + (H_C^2)_{i-1}^n}{(\triangle\xi)^2} - \frac{\beta}{\epsilon}[(H_B^2)_i^n - (H_C^2)_i^n]. \tag{64}$$

These correspond to

$$(H_B)_i^{n+1} = s_B[(H_B^2)_{i+1}^n - 2(H_B^2)_i^n + (H_B^2)_{i-1}^n] - \triangle\theta\beta[(H_B^2)_i^n - (H_C^2)_i^n], \tag{65}$$

$$(H_C)_i^{n+1} = s_C[(H_C^2)_{i+1}^n - 2(H_C^2)_i^n + (H_C^2)_{i-1}^n] - \frac{\triangle\theta\beta}{\epsilon}[(H_B^2)_i^n - (H_C^2)_i^n], \tag{66}$$

where $i = 2, ..., N$, $s_B = \frac{\kappa_B}{\kappa_C} \frac{\triangle\theta}{(\triangle\xi)^2}$ and $s_C = \frac{\triangle\theta}{(\triangle\xi)^2}$.

The first cell $i = 1$ and the last cell $i = N + 1$ are the boundary value

$$H_B(1, k) = H_C(1, k) = 0,$$
$$H_B(N + 1, k) = H_C(N + 1, k) = 0.$$

The initial states of the scheme are followed by equations

$$(H_B)_i^1 = \frac{\kappa_B}{\kappa_C} s_B[(H_B^2)_{i+1}^0 - 2(H_B^2)_i^0 + (H_B^2)_{i-1}^0] - \triangle\theta\beta[(H_B^2)_i^0 - (H_C^2)_i^0], \tag{67}$$

$$(H_C)_i^1 = s_C[(H_C^2)_{i+1}^0 - 2(H_C^2)_i^0 + (H_C^2)_{i-1}^0] - \frac{\triangle\theta\beta}{\epsilon}[(H_B^2)_i^0 - (H_C^2)_i^0], \tag{68}$$

where $H_B^2(\cdot, 0)$, $H_C^2(\cdot, 0)$ are the initial distributions of the porous blocks and the system fissures.

3.4 Model results

3.4.1 Procedure of the computational

The discrete schemes 65-66 are simulated with dimensionless space $\xi \in [0, 10]$ and dimensionless time $\theta \in [0, 2000]$ and a short interval dimensionless time $\theta \in [-1, 0]$ before time goes to zero at the boundary $\xi = 0$. The number of cells is $N + 1 = 501$.

The porous blocks discrete scheme 65 has a frozen coefficient that $\frac{\kappa_B}{\kappa_C} = 10^{-4}$ is considered, so the parameters of the discrete equations are $s_B \ll s_C$,

$$s_B = \frac{\kappa_B}{\kappa_C}\frac{\triangle\theta}{(\triangle x)^2} = 10^{-4}\frac{0.01}{0.02^2} = 2.5 \cdot 10^{-3},$$
$$s_C = \frac{\triangle\theta}{(\triangle x)^2} = 25.$$

The values of the parameters $\beta = 10^{-2}$ and $\epsilon = 10^{-4}$ are taken in computational.

The procedure of computational experiment begins with the same as the homogeneous porous medium. Firstly, the intense pulse of porous blocks at the boundary is obtained from the dimensionless function $f(\theta)$ when time is less than zero. In this moment,the exchange flow does not appear between two embedded porous media. The relationship between the porosity of the porous blocks and system cracks is the ratio ϵ, so the pulse of the system cracks is also defined such as

$$H_C(0, t < 0) = \epsilon H_B(0, t < 0). \tag{69}$$

Next, the initial state ($\theta < 0$) is computed with the same form explicit schemes 65-66 with the boundary profile and the initial data is equivalent to zero.

The initial water level of porous blocks and system cracks are updated at $\theta = 0$. Thus, the numerical schemes 65-66 are simulated to get the results for porous blocks and system cracks.

3.4.2 Numerical modelling results

A profile of water level at the boundary is defined using function $f(\theta)$ with $\theta_* = -0.80$ in figure 19. The maximum of dimensionless water level reaches $H = 1.00$ at constant dimensionless time $\theta_* = -0.80$. The initial distribution at $\theta = -1$ is assumed to zero.

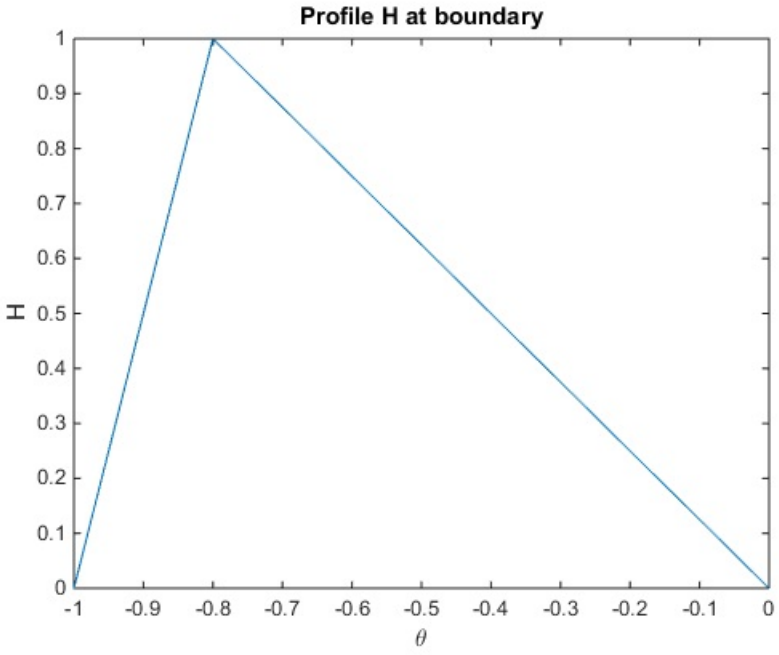

Figure 19: Profile of the water height at the boundary from $\theta = -1.00$ to $\theta = 0$ with $\theta_* = -0.80$.

Following the procedure, the initial distribution for large times case at $\theta = 0$ is defined as the figures 20 and 21 for fissurized porous blocks and system cracks. In these figures, the relation between the water levels of porous blocks and system cracks are the ratio of two porosity $\epsilon = 10^{-4}$. The initial distribution in purely porous blocks is also defined in figure 22, the height is lower than in the fractured porous blocks and the position of front is shorter than in the system cracks.

After that, the discrete schemes 65-66 are computed and show the results in figures 23, 24 and 25. The water levels of porous blocks $H_B(x, \theta)$ (dash line) and system cracks $H_C(x, \theta)$ (solid line) are distributed for time $\theta = 10.00$, $\theta = 100.00$ and $\theta = 1000.00$. The water level of the porous blocks is higher than the system cracks, but the front position of system cracks goes faster than the front of porous blocks to extent into the media.

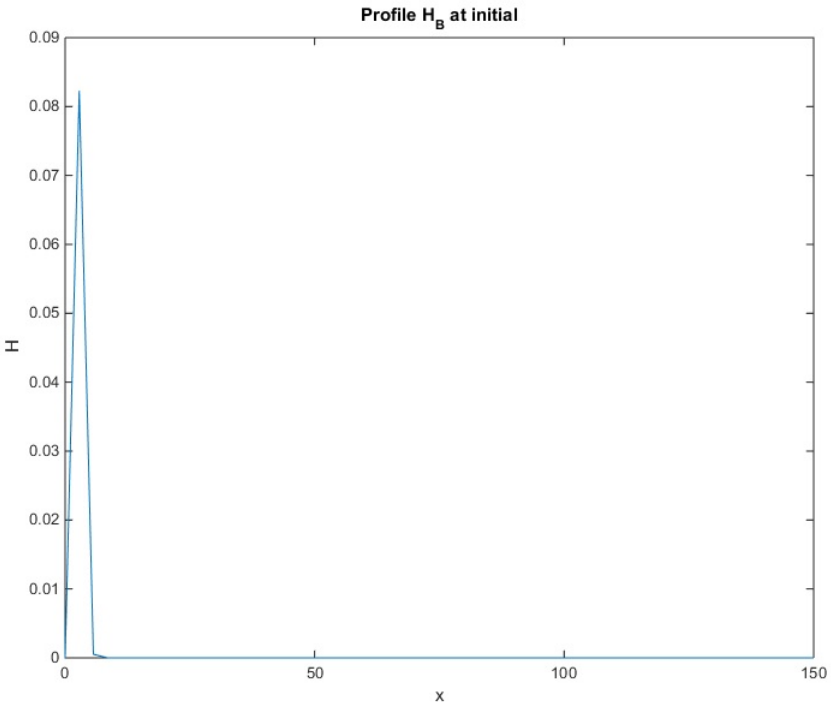

Figure 20: The initial distribution at $\theta = 0$ in fissurized porous blocks.

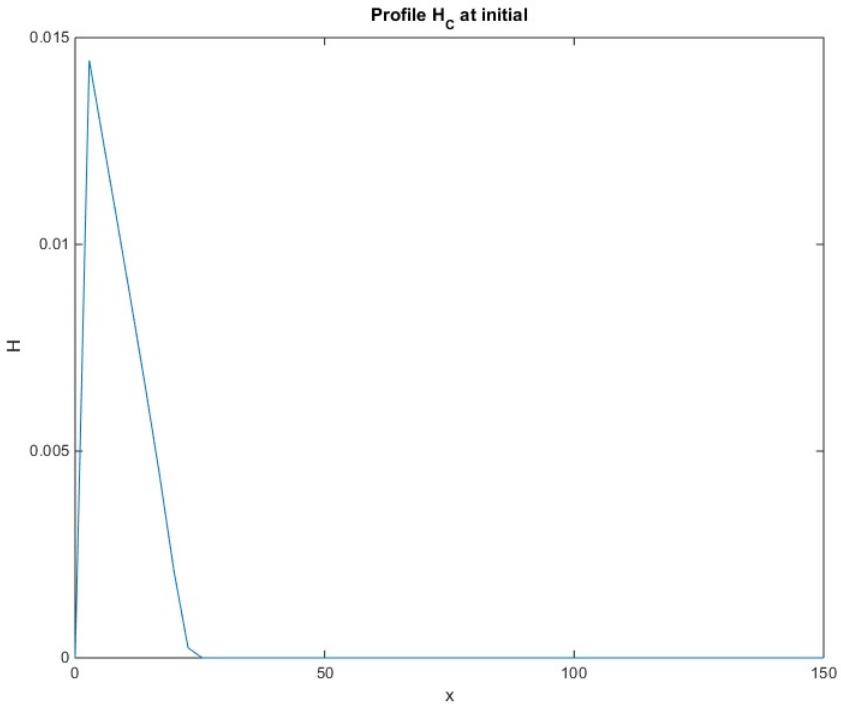

Figure 21: The initial distribution at $\theta = 0$ in system cracks.

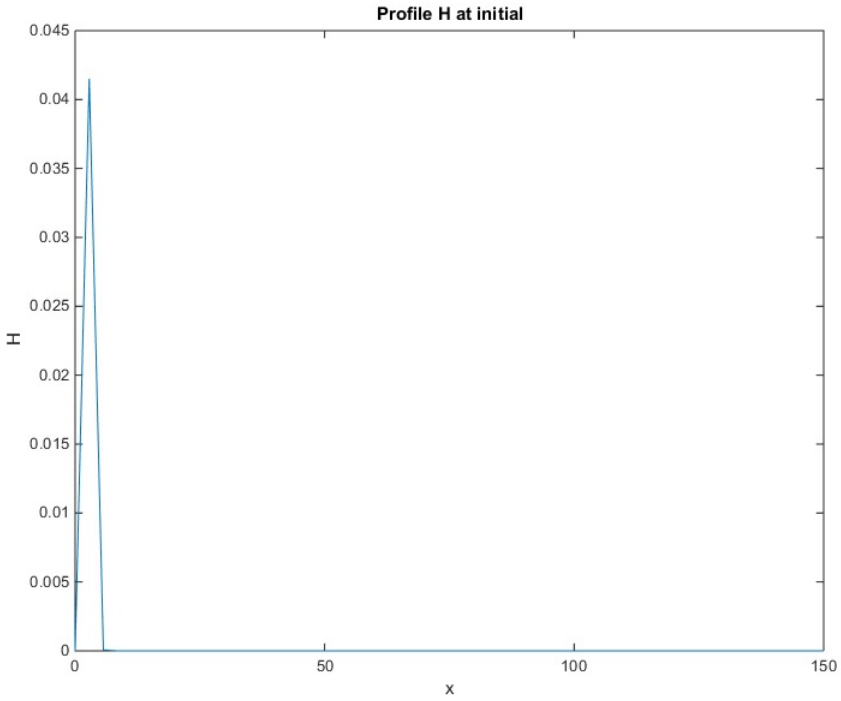

Figure 22: The initial distribution at $\theta = 0$ in purely porous blocks.

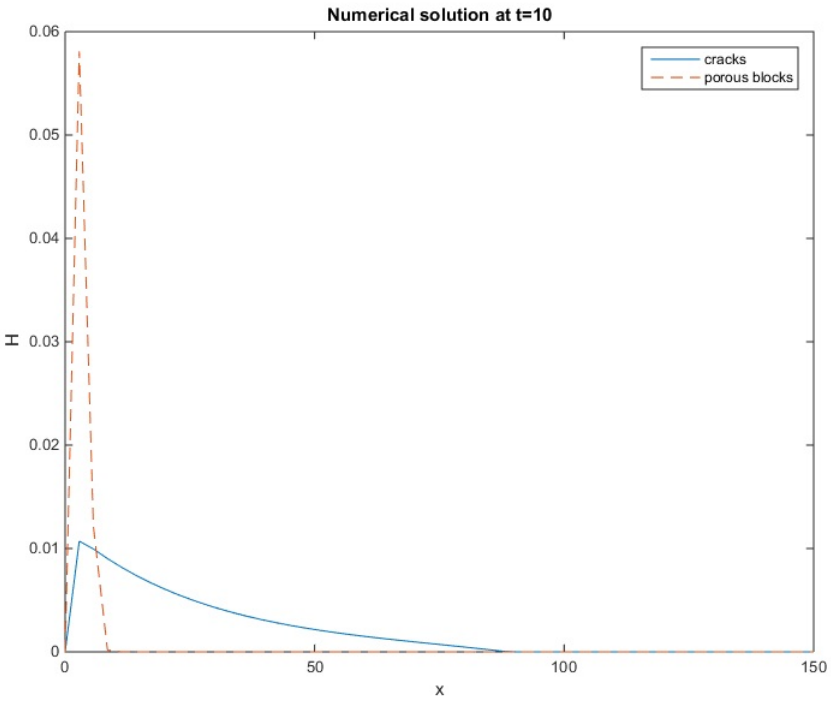

Figure 23: The water level in fissurized porous blocks and cracks at $t = 10.00$. The water level $h_B(x, t = 10.00)$ (red dash line) is higher than the water level $h_C(x, t = 10.00)$ (blue line), but system cracks extension is faster.

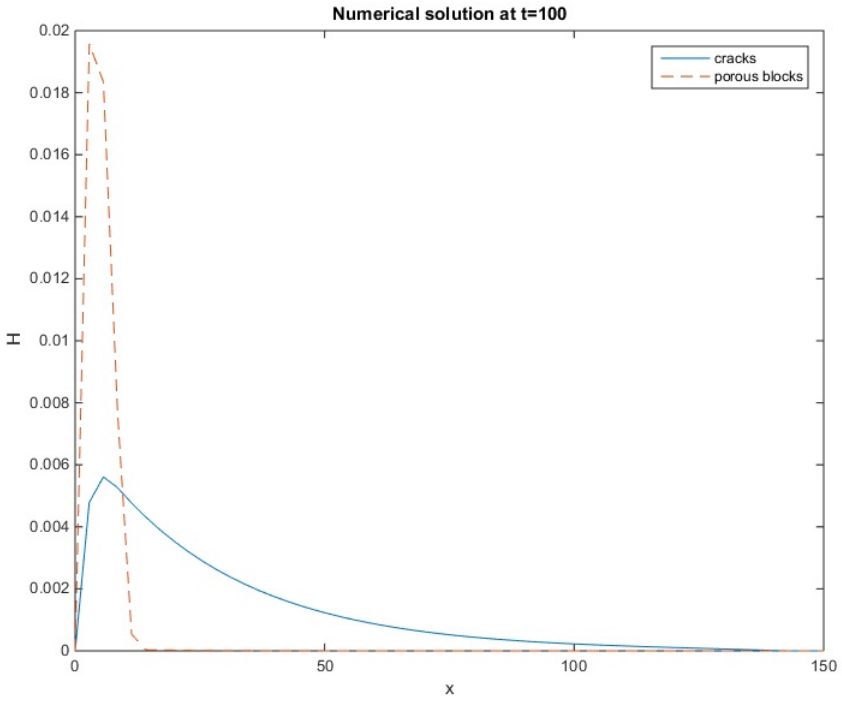

Figure 24: The water level in fissurized porous blocks and cracks at $t = 100.00$. With increasing time, the heights are lower and the extensions are further.

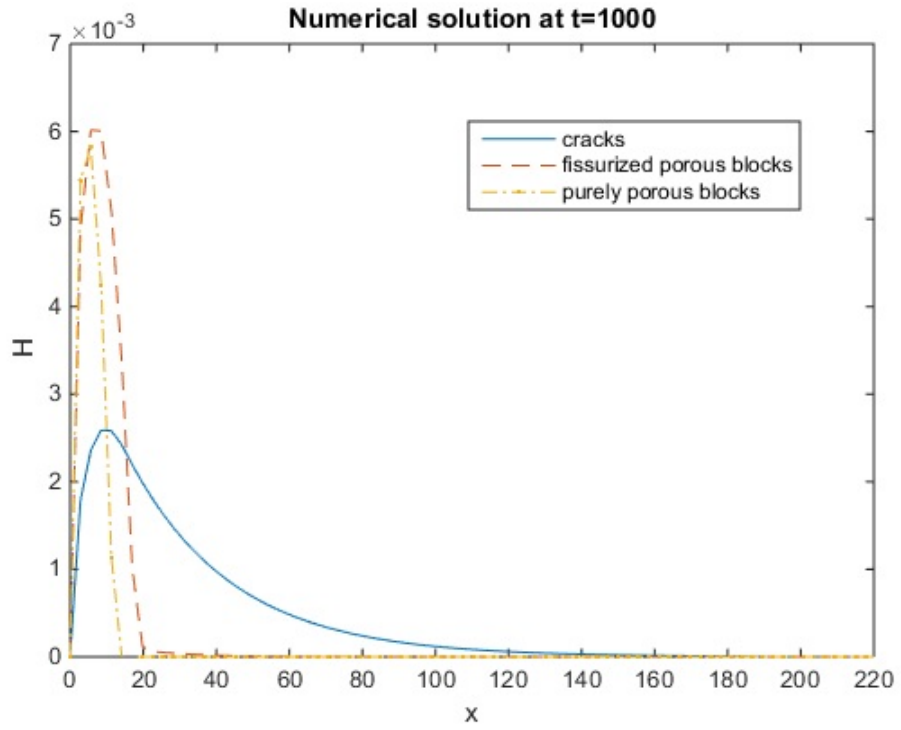

Figure 25: The water level in purely porous blocks, fissurized porous blocks and cracks at $t = 1000.00$. The mass of fluid and the front position of flow in purely porous blocks are less than in fissurized porous blocks.

Checking of the results The front of groundwater mound, which is observed from time $t = 10.00$ in figure 23 will be checked with the theory to get a accuracy of the numerical method. At the initial distribution, $\theta = \theta_0 = 0$, the flow has the front at $\xi_f = \xi_{f0}$. The distribution of groundwater levels near $\xi = \xi_{f0}$ are assumed as a steady one after a short time interval near $\theta = 0$. The dimensionless velocity of the fluid tongue extension is considered as a constant and has the rate [1]

$$V = \frac{d\xi_f}{d\theta} = \frac{\xi_f - \xi_{f0}}{\theta - \theta_0} = \frac{\xi_f - \xi_{f0}}{\theta} = constant. \tag{70}$$

The functions of water height near the front are in the forms [1]

$$\begin{aligned} H_B &= H_B(\zeta), \\ H_C &= H_C(\zeta), \\ \zeta &= \xi - V(\theta - \theta_0) - \xi_{f0}. \end{aligned}$$

When ζ is near zero, the front is $\xi = \xi_f = \xi_{f0} + V(\theta - \theta_0)$. Equations 65 and 66 are returned to the same functions of ζ as the forms

$$\begin{aligned} \frac{d}{d\zeta}\frac{d\zeta}{d\theta}H_B &= \frac{\kappa_B}{\kappa_C}\frac{d^2}{d\zeta^2}\frac{d\zeta^2}{d\xi^2}H_B^2 - \beta(H_B^2 - H_C^2), \\ \frac{d}{d\zeta}\frac{d\zeta}{d\theta}H_C &= \frac{d^2}{d\zeta^2}\frac{d\zeta^2}{d\xi^2}H_C^2 + \frac{\beta}{\epsilon}(H_B^2 - H_C^2). \end{aligned}$$

Derivation of $\frac{d\zeta}{d\theta}$ and $\frac{d\zeta^2}{d\xi^2}$ are calculated such as

$$\begin{aligned} \frac{d\zeta}{d\theta} &= \frac{d(\xi - V(\theta - \theta_0) - \xi_{f0})}{d\theta} = -V, \\ \frac{d\zeta^2}{d\xi^2} &= \frac{d(\xi - V(\theta - \theta_0) - \xi_{f0})^2}{d\xi^2} = \frac{d\xi^2}{d\xi^2} = 1. \end{aligned}$$

Now, the equations 65 and 66 are in the following forms

$$V\frac{d}{d\zeta}H_B + \frac{\kappa_B}{\kappa_C}\frac{d^2}{d\zeta^2}H_B^2 - \beta(H_B^2 - H_C^2) = 0, \tag{71}$$

$$V\frac{d}{d\zeta}H_C + \frac{d^2}{d\zeta^2}H_C^2 + \frac{\beta}{\epsilon}(H_B^2 - H_C^2) = 0. \tag{72}$$

The terms $\frac{\kappa_B}{\kappa_C}\frac{d^2}{d\zeta^2}H_B^2$ and βH_B^2 in equation 71 can be neglected. So, the equation takes the form

$$V\frac{d}{d\zeta}H_B + \beta H_C^2 = 0. \tag{73}$$

From the reference [1], the behavior of the function $H_C(\zeta)$ is a linear one near $\zeta = 0$, $H_C(\zeta) = -A\zeta$, where A is a certain positive constant. The function of $H_B(\zeta)$ is computed from equation 73,

$$\begin{aligned}
V\frac{d}{d\zeta}H_B + \beta A^2\zeta^2 &= 0,\\
\int V dH_B &= -\int \beta A^2\zeta^2 d\zeta,\\
VH_B &= -\frac{\beta A^2}{3}\zeta^3,\\
H_B &= -\frac{\beta A^2}{3V}\zeta^3,\\
H_B &= \frac{\beta}{3AV}H_C^3,\\
H_B^{1/3} &= (\frac{\beta}{3AV})^{1/3}H_C.
\end{aligned}$$

Therefore, near $\zeta = 0$, i.e. $\xi = \xi_f$, the proportional of $H_B^{1/3}$ to H_C is in the form $H_B^{1/3} = (\beta/3AV)^{1/3}H_C$.

In the figure 26 and 27, the water heights in fissurized porous blocks and system cracks are plotted in the same scale in x-direction. The water heights have a linear shape at the front $x_f(t)$ and the proportional between them is

$$\begin{aligned}
H_B^{1/3} &\propto H_C,\\
10^{-15/3} &\propto 10^{-6}.
\end{aligned}$$

With $\beta = 10^{-2}$ and $A = 10^{-4}$ are assumed, the dimensionless velocity of the front is $V = 2.00 \cdot 10^{-3}$. This velocity is used to calculate the front of the flow in fissurized porous medium in the next section.

$$\begin{aligned}
(\frac{\beta}{3AV})^{1/3} = \frac{H_B^{1/3}}{H_C} = \frac{(5.20 \cdot 10^{-15})^{1/3}}{0.68 \cdot 10^{-6}} &= 25.48,\\
\frac{\beta}{3AV} &= 16542.40,\\
V = \frac{10^{-2}}{3 \cdot 10^{-4} \cdot 16542.40} &= 2.00 \cdot 10^{-3}.
\end{aligned}$$

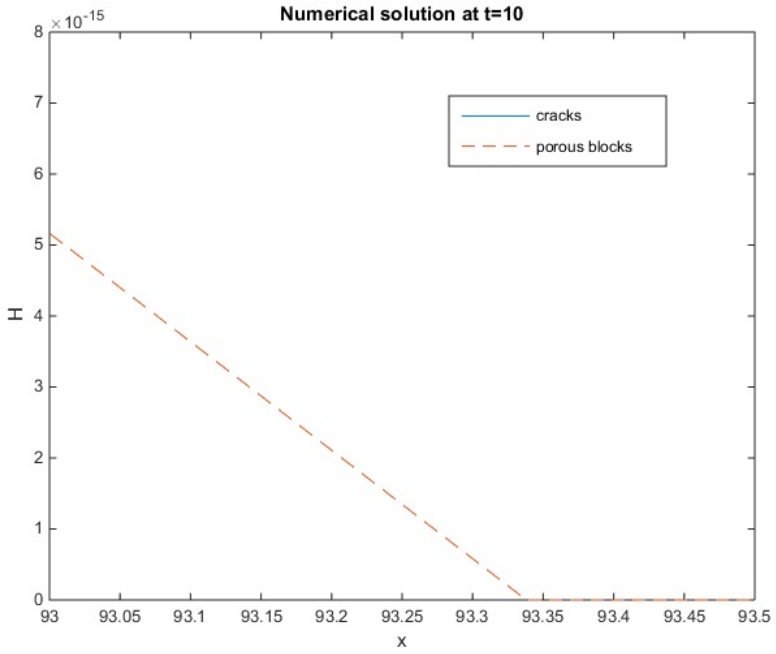

Figure 26: The water level near the front in fissurized porous blocks at $t = 10.00$.

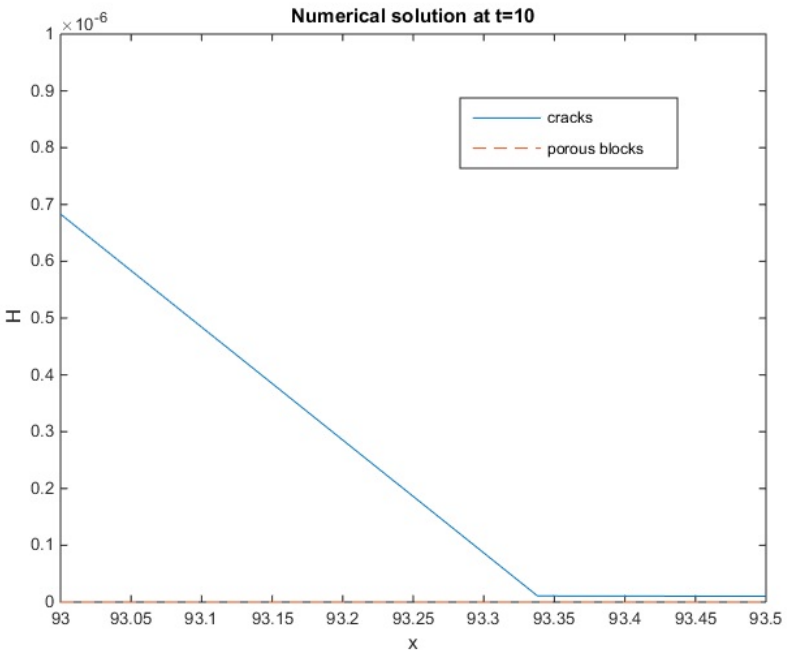

Figure 27: The water level near the front in system cracks at $t = 10.00$.

4 Comparison on the results in purely and fissurized porous blocks

When the homogeneous and heterogeneous porous medium is compared, the properties are changed because the REV are larger to get the different models from the figure 6. Therefore, the coefficient in the model of homogeneous porous medium is smaller than in heterogeneous porous medium, $\kappa_p = \kappa_B/2 = 0.20/2 = 0.10$.
The model for purely porous medium is

$$\partial_\theta H_p = \frac{\kappa_p}{\kappa_C}\partial^2_{\xi\xi} H_p^2 - \beta H_B^2. \tag{74}$$

The discrete scheme is in the form

$$(H_p)_i^{n+1} = \frac{\kappa_p}{\kappa_C} s_B[(H_p^2)_{i+1}^n - 2(H_p^2)_i^n + (H_p^2)_{i-1}^n] - \triangle\theta\beta(H_B^2)_i^n. \tag{75}$$

The initial distribution has the scheme equation

$$(H_p)_i^1 = \frac{\kappa_p}{\kappa_C} s_B[(H_p^2)_{i+1}^0 - 2(H_p^2)_i^0 + (H_p^2)_{i-1}^0] - \triangle\theta\beta(H_B^2)_i^0. \tag{76}$$

The numerical scheme is simulated and compared in the figure 25 at time $t = 1000.00$. The mass of fluid in purely porous blocks without the system cracks is smaller than fissurized porous blocks. The front does not move further as in fissurized porous blocks.

The figure 28 represents a large dipole moment is concentrated in porous blocks. The maximum heigh t breakthrough boundary is h_0 at a short time interval $\theta = 1.00$. The dipole moment is calculated from that height is a maximum energy and this energy is conserved such as the dipole moment is a constant. Dipole moment of system cracks also has a maximum energy at boundary, but it decreases in transient flow at short time interval $\theta = 1.00$ and comes to a constant from $\theta = 0$.

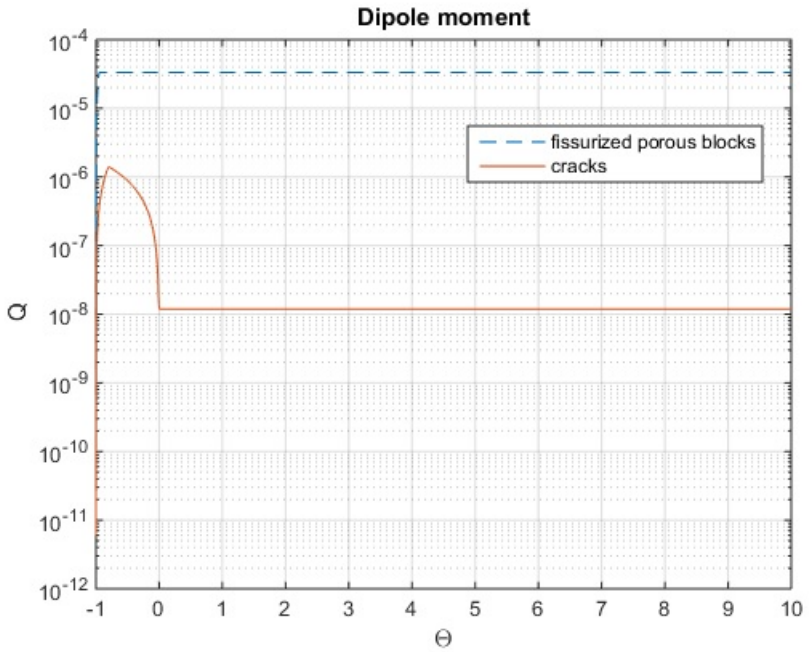

Figure 28: The dipole moment Q in fissurized porous blocks and cracks. A major part of dipole moment is contained in fissurized porous blocks.

The bulk fluid mass is defined from density of water, $\rho = 997kg/m^3$, multiply by dipole moment Q, which is assumed to a volumetric flow rate per unit width. The result in figure 29 represents the total mass of fluid in porous blocks and system cracks. The mass of fluid in porous blocks is a major part of the fluid in fissurized porous medium.

The front position $x_f(\theta)$ is represented in figure 30. The front of

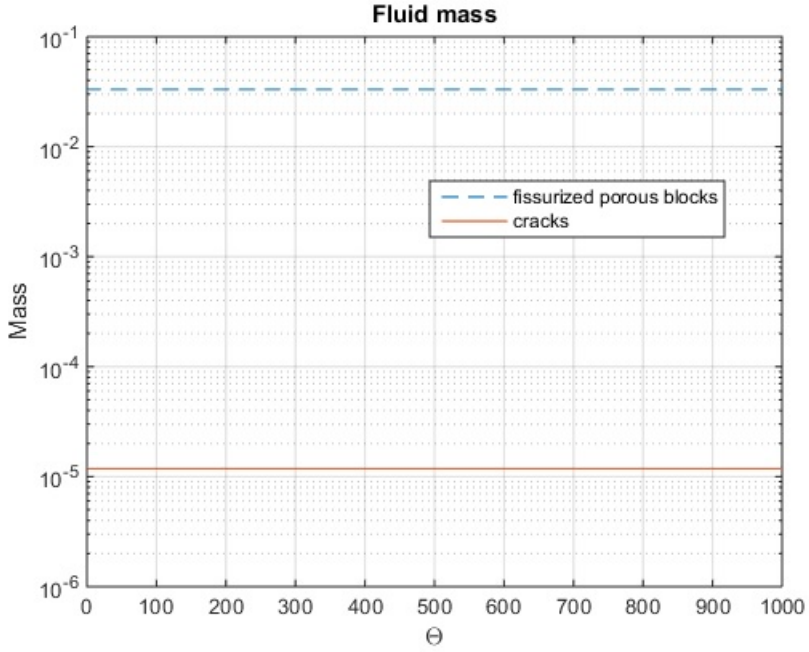

Figure 29: The bulk mass of the fluid movement. A major part of mass concentrates in fissurized porous blocks.

groundwater flow in fissurized porous medium is calculated by

$$x_f^{fissure}(\theta) = x_{f0} + [V(\theta - \theta_0)]\sqrt{\kappa_C h_0 \tau}, \tag{77}$$

where $V = 2.00 \cdot 10^{-3}$, $x_{f0} = 34.00$ at the initial $\theta_0 = 0$ and the height $h_0 = 10.00$. The groundwater dome extension in purely porous medium is computed from the following equation

$$x_f^{purely}(\theta) = [2(5\kappa_p Q_p \theta)^{1/4}]\sqrt{\kappa_C h_0 \tau}. \tag{78}$$

The groundwater mound reaches boundary $x^*(t)$ when $h_B(x^*, t) = h_C(x^*, t)$. The function $x^*(t)$ is the extension of the zone where water level in porous blocks is higher than in system cracks [1] and is computed by different dipole moment in porous blocks and in system cracks by the following equation

$$x_f^*(\theta) = [2(5\kappa_B(Q_B - Q_C)\theta)^{1/4}]\sqrt{\kappa_C h_0 \tau}. \tag{79}$$

The groundwater fronts are plotted in figure 30. The results indicate that the front position in fissurized porous blocks extends faster than in purely porous blocks. The boundary $x^*(t)$ is nearly same with the front in homogeneous porous blocks.

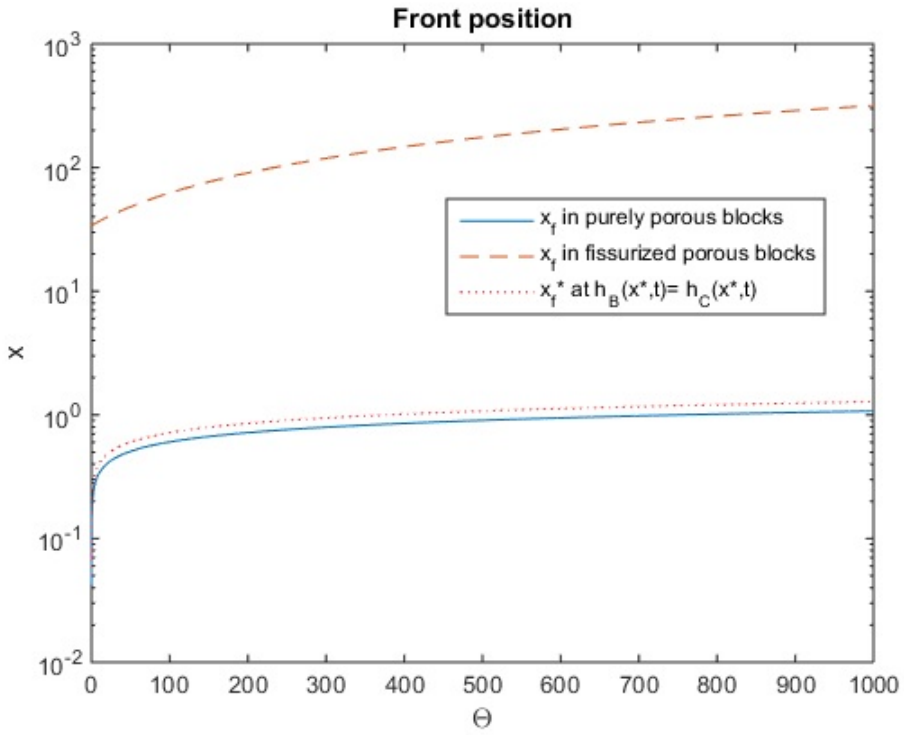

Figure 30: The front positions of the groundwater flow. The front of flow in fissurized porous medium (dash line) extents faster than in purely porous medium (blue line). The boundary at $x^*(t)$ (dot line) is closer with the front in purely porous medium.

5 Summary and conclusion

The problem of the flow in porous medium is considered in two models: one in homogeneous porous blocks and one in fissurized porous blocks with a system cracks. The boundary and initial values are different with time $-t$ and $+t$. When time is negative $[-\tau, 0]$, a short time interval $t = \tau$, the groundwater flow is an intense pulse at the boundary $x = 0$ that is used to obtained the initial distribution at large positive times $t = T$. The models have the initial distribution and the boundary is zero at $x = 0$ and at infinite because the length of porous medium is considered semi-infinite.

The models are simulated at large times, so the groundwater flow has form as the mound with water height of saturated region and the front of the flow indicates extension into porous medium. The mathematical models is computed with the input parameters in table 3. The purely porous blocks is computed under the same conditions with the fissurized porous blocks for comparison.

Input	Homogeneous	Porous blocks	Cracks	Purely Porous blocks
κ	0.20	0.20	2000	0.10
Length, L	100.00	10.00	10.00	10.00
Time, T	2000	2000	2000	2000
τ	1.00	1.00	1.00	1.00
Cells, $N + 1$	501	501	501	501

Table 3: The input parameters.

The output parameters are the water level in figures 23-25, dipole moment Q in table 4 and the front of the groundwater mound in figure 30. The water height decrease with larger times at all cases. The dipole moment is a constant from time is zero. The constancy dipole moment gives a self-similar solution for exact analytically and a stability estimation for numerical solution. The front position indicates that a penetration of flow in stratified heterogeneous medium is more than in homogeneous porous medium because a system fissures supports the groundwater flow near the front.

Output	Homogeneous	Porous blocks	Cracks	Purely Porous blocks
Q	6.67	$3.33 \cdot 10^{-5}$	$1.19 \cdot 10^{-8}$	$1.67 \cdot 10^{-5}$

Table 4: Dipole moment from computational.

The results from the mathematical models proposed above in this studying give us the following conclusions.

- The flow in porous medium is affected by the fissures dramatically. The mass of fluid of the groundwater breakthrough the boundary is larger such as the height and speed of penetration of the fluid.

- The water distribution in porous blocks and system cracks has two regions: one near the boundary is blocks-dominated, where the water level in porous blocks is larger then in system cracks, and a fissures-dominated region near the front where the water level in system cracks is larger than in porous blocks. This conclusion is same with the conclusion from Barenblatt et al. (1999) [1].

- The concept of the exchange flow between porous blocks and fissures at any fixed place is at first the fissures feed the porous blocks when the groundwater enters the medium. Secondly, the porous blocks start to feed the fissures to support the water level of saturated part of the medium via the fissures. This is an explanation for a double porous medium behavior that the fluid is produced into well by a higher permeability medium (or a system fissures) and a lower permeability medium (or porous blocks) recharges for a higher permeability medium.

- A major part of the mass of fluid enters the medium is concentrated in the porous blocks. The fissures affect largely on the penetration of the fluid into the medium. When computing of the contamination, the fissures have to take into account to correct the evolution in fissurized rocks.

List of Symbols

A	a positive constant
α	exchange coefficient
β	dimensionless exchange coefficient
ϵ	ratio of system cracks porosity and porosity of porous blocks
g	acceleration of gravity
h	water level of homogeneous porous blocks
h_0	maximum water level
H_B	dimensionless water level of porous blocks
H_C	dimensionless water level of system cracks
k	permeability of homogeneous porous blocks
k_B	permeability of fissurized-porous blocks
k_C	permeability of system cracks
κ	coefficient of the Boussinesq equation for homogeneous porous blocks
κ_B	coefficient of the Boussinesq equation for porous blocks
κ_C	coefficient of the Boussinesq equation for system cracks
κ_p	coefficient of the Boussinesq equation for purely porous blocks
L	length of porous medium
M	dimensionless dipole moment of fissurized porous blocks
m	porosity of porous blocks
μ	viscosity of fluid
Q	dipole moment of homogeneous porous blocks
Q_B	dipole moment of porous blocks
Q_C	dipole moment of system cracks
ρ	density of fluid
T	total time
t	time
τ	short time interval at the boundary
θ	dimensionless time
θ_0	short dimensionless time interval near a steady flow
V	dimensionless velocity of fluid tongue extension

x	position
x_f	front position of groundwater mound
ξ	dimensionless position
ξ_f	dimensionless front position
ξ_{f0}	dimensionless front position near a steady flow at short dimensionless time θ_0

x, x_f, t, L, h, h_0, H_B, H_C, ξ, ξ_f,ξ_{f0}, θ, κ, κ_B, κ_C, κ_p, ρ, m, g, μ, k,k_B, k_C, Q, Q_B, Q_C, M, A, V, α, β, ϵ, T, τ, θ_0

List of Figures

List of Tables

References

[1] G. I. Barenblatt, E. A. Ingerman, H. Shvets, and J. L. Vazquez, "Very intense pulse in the groundwater flow in fissurized-porous stratum," *Proceedings of the National Academy of Sciences of the United States of America*, vol. 97, no. 4, pp. 1366–1369, 2000.

[2] J. Boussinesq, "Therie analytiche de la chaleur mise en harmonie avec la thermodynamique et avec la thorie mcanique de la lumire," *Monatshefte fr Mathematik und Physik*, vol. 14, pp. A11–A12, December 1903.

[3] MrRateeb, "recognize double porosity system from well tests." https://www.slideshare.net/MrRateeb/recognize-double-porosity-system-from-well-tests, Nov. 2012. Published in: Education.

[4] G. Barenblatt, "Theory of fluid flows through natural rocks," vol. 3, 1990.

[5] G. Barenblatt, I. P. Zheltov, and I. Kochina, "Basic concepts in the theory of seepage of homogeneous liquids in fissured rocks [strata]," *Journal of applied mathematics and mechanics*, vol. 24, no. 5, pp. 1286–1303, 1960.

[6] P. Y. Polubarinova-Kochina, "Theory of groundwater movement," *Princeton Univ. Press, Princeton*, 1962.

[7] J. Bear, *Dynamics of fluids in porous media*. Dover books on physics and chemistry, New York: Dover, 1988.

[8] Wikipedia, "Permeability (earth sciences)." `https://en.wikipedia.org/wiki/Permeability_(earth_sciences)`, Mar. 2018.

[9] D. L. Turcotte and G. Schubert, *Geodynamics*. Cambridge: Cambridge University Press, 2nd ed. ed., 2002.

[10] V. Lampe, "Modelling fluid flow and heat transport in fractured porous media," 2013.

[11] M. Rouse, "gravitational acceleration." `https://whatis.techtarget.com/definition/gravitational-acceleration`, Sept. 2005.

[12] A. Tveito, *Introduction to partial differential equations : a computational approach*, vol. 29 of *Texts in applied mathematics*. New York: Springer, 1998.

[13] G. Barenblatt and J. Vazquez, "A new free boundary problem for unsteady flows in porous media," *European Journal of Applied Mathematics*, vol. 9, no. 1, pp. 37–54, 1998.

[14] Y. B. Zeldovich and G. Barenblatt, "On the dipole-type solution in the problems of a polytropic gas flow in porous medium," *Prikl. Mat. Mekh*, vol. 21, pp. 718–720, 1957.

[15] J. S. Mathunjwa and A. J. Hogg, "Freely draining gravity currents in porous media: dipole self-similar solutions with and without capillary retention," *European Journal of Applied Mathematics*, vol. 18, no. 3, pp. 337–362, 2007.

[16] Z.-X. Chen, "Transient flow of slightly compressible fluids through double-porosity, double-permeability systems — a state-of-the-art review," *Transport in Porous Media*, vol. 4, pp. 147–184, Apr 1989.

[17] U. Svensson, "A continuum representation of fracture networks. part i: Method and basic test cases," *Journal of Hydrology*, vol. 250, no. 1, pp. 170 – 186, 2001.

Appendix A: MATLAB code for the homogeneous porous medium

Note: The code for the homogeneous porous medium is completed in cooperation with YangYang Qiao, who is the Research Fellow at University of Stavanger.

```
clear;
% The model for homogenous porous medium
%Define function f(theta)
thetastar = -0.3; % a constant dimensionless time
deltat = 0.01;
theta0 = -1 : deltat : 0 ; % time theta0=[-1,0]
h0 = 10;

for i = 1 : (1/deltat + 1) %time loop
if theta0(i) < thetastar
f(i) = h0 * (theta0(i) + 1)/(thetastar + 1) ;
else
f(i) = h0 * theta0(i)/thetastar ;
end
end

plot(theta0,f)
title('Profile h at boundary')
xlabel('t')
ylabel('h')
pause

%----------grid----------
L = 100.; % Length of the wire
T = 2000.; % Total time
Ntime = T * 100; % Number of time steps
dt = T/Ntime;
N = 500; % Number of cells
dx = L/N;
kappa = 2e - 05 * 10000;
b = dt/(dx * dx);
s = b * kappa % Stability parameter for explicit method
------------------------------
```

% Water level at the boundary H(0,theta)= f(theta)

for $k = 1 : Ntime + 1$ %time loop
%left boundary at x=0
if $k < (1/deltat + 1)$
$u(1, k) = f(k)$;
else
$u(1, k) = 0$;
end
$u(N + 1, k) = 0.$;
$time(k) = (k - 1) * dt - 1$; %define real time
end

% Define initial data using explicit method
% Numerical scheme for short time interval

for $k = 1 : 1/deltat$ % Time Loop
for $i = 2 : N$ % Space Loop
$u(i, k+1) = u(i, k) + s * (u(i-1, k).^2 + u(i+1, k).^2 - 2. * u(i, k).^2)$;
end
end

%define dipole moment Q at time t=0
$Q = 0$;

for $i = 1 : N + 1$ %Space loop
$x(i) = (i - 1) * dx$;%define real position x
$Q = Q + (x(i) * u(i, 1/deltat + 1) * dx)$;
$U(i, 1) = u(i, 1/deltat + 1)$; % Update initial state
end

plot(x,u(:,1/deltat+1))
title('Profile h at initial')
xlabel('x')
ylabel('h')
axis([0 100 0 10])
pause
%———-Analytical solution————————
$zeta0 = 2.99$;

for $k = 1/deltat + 2 : Ntime$
$xf(k) = (Q * coeff * (time(k) + 1))^(1/4) * zeta0;$
$record(k) = ceil(xf(k)/dx);$
end

---

for k=1/deltat+2:Ntime
for i=1:record(k)
zeta(i,k)=x(i)/xf(k);
if zeta(i,k)¡=zeta0
$Phi(i,k) = (5^0.5/3) * zeta(i,k)^0.5 * (1 - zeta(i,k)^1.5);$
else
$Phi(i,k) = 0;$
end
$h(i,k) = ((Q/(coeff * (time(k) + 1)))^0.5) * Phi(i,k);$
end
end
%————————Plot the exact anaytical results————————
y1=102; y2=202; y3=302; y4=402;
K1=1002; K2=2002; K3=3002; K4=4002;
figure(1)
plot(x,u(:,1/deltat+1),x(1:record(y1)),h(1:record(y1),y1)
,x(1:record(y2)),h(1:record(y2),y2),x(1:record(y3)),h(1:record(y3),y3)
,x(1:record(y4)),h(1:record(y4),y4),x(1:record(K1)),h(1:record(K1),K1)
,x(1:record(K2)),h(1:record(K2),K2),x(1:record(K3)),h(1:record(K3),K3)
,x(1:record(K4)),h(1:record(K4),K4))
title('Analytical solution for homogeneous porous media')
xlabel('x')
ylabel('h')
axis([0 10 0 4])
legend('t=0','t=10','t=20','t=30','t=40','t=100',
't=200','t=300','t=400')

% ————————NUMERICAL SCHEME————————————————
for k=1:Ntime
for i=2:N;
$U(i,k+1) = U(i,k)+s*(U(i-1,k).^2+U(i+1,k).^2-2.*U(i,k).^2);$
end
$U(1,k) = 0;$
$U(N+1,k) = 0.;$
end

```
%————————Plot the numerical result————————————-
figure(2)
plot (x,U(:,1),x,U(:,y1),x,U(:,y2),x,U(:,y3) ,x,U(:,y4),
x,U(:,K1),x,U(:,K2),x,U(:,K3),x,U(:,K4))
title('Numerical solution for homogeneous porous media')
xlabel('x')
ylabel('h')
axis([0 10 0 4]) legend('t=0','t=10','t=20','t=30','t=40',
't=100','t=200','t=300','t=400')
```

Appendix B: MATLAB code for the heterogeneous porous medium

```
clear;
        %the model for heteregenous porous medium
        %Define dimensionless function f(theta)
        thetastar= -0.8; %a constant dimensionless time
        deltat=0.01;
        theta=-1:deltat:0 ; % dimensionless time interval θ = [−1, 0]

        for i=1:(1/deltat+1)
        if theta(i) < thetastar
        f(i) = (theta(i)+1)/(thetastar+1);
        else
        f(i) = theta(i)/thetastar ;
        end
        end

        plot(theta,f)
        title('Profile H at boundary')
        xlabel('t')
        ylabel('H')

        %——grids of modelling————————————
        L = 10.; % Length of the wire
        T =2000.; % Total time
        Ntime = T*100; % Number of time steps
        dt = T/Ntime;
        N=500; %Number of cells
        dx = L/N;
        %————————-input parameters————————————————
        kappaB = 0.2; % coefficient of porous blocks
        kappaC=2000; % coefficient of cracks
        kappa=kappaB/2; % coefficient of purely porous blocks
        b = dt/(dx*dx);
        sB=b*(kappaB/kappaC) % parameter of porous blocks
        sC= dt/(dx*dx) % parameter of system cracks
        s=b*(kappa/kappaC) % parameter of purely porous blocks
        beta=1e-02; % the exchange coeff epsilon=1e-04; % the ratio of
two porosity =mc/mb
```

pause
%————————Boundary condition————————————
% Water level at the boundary H(0,theta)= f(theta)
for k=1:Ntime+1 %time loop
%left boundary at x=0
if $k < (1/deltat + 1)$
hb(1,k) = f(k);

u(1,k) = f(k);

else

hb(1,k) =0 ; u(1,k) =0 ;
end
hb(N+1,k) = 0.;
time(k) = (k-1)*dt-1; %define real time

u(N+1,k) = 0.;
end
$hc = hb * epsilon$; % Define initial state hc(t¡0)
u=hb; % Define initial state for homogeneous porous blocks
h0=10;

for i=1:N+1
$x(i) = (i-1)*dx*sqrt(h0*kappaC)$; %define real position x (h0=10, tau=1)
end
%————————————-Initial state————————————
for k=1:1/deltat % Time Loop
for i=2:N % Space Loop
% the discrete scheme for a short time interval tau=1
$hb(i,k+1) = hb(i,k) + sB * (hb(i-1,k).^2 + hb(i+1,k).^2 - 2. * hb(i,k).^2) - dt * (hb(i,k).^2 - hc(i,k).^2) * beta$;
$hc(i,k+1) = hc(i,k) + sC * (hc(i-1,k).^2 + hc(i+1,k).^2 - 2. * hc(i,k).^2) + dt * (hb(i,k).^2 - hc(i,k).^2) * (beta/epsilon)$;
$u(i,k+1) = u(i,k) + s * (u(i-1,k).^2 + u(i+1,k).^2 - 2. * u(i,k).^2) - dt * (hb(i,k).^2) * (beta)$;
end
end

Qb=0; Qc=0; Q=0; Qhomo=0;
for i = 1:N+1 %Space loop

%define dipole moment Q at time t=0

$Q = Q + (x(i) * (hb(i, 1/deltat + 1) + epsilon * hc(i, 1/deltat + 1)) * dx/sqrt(h0 * kappaC))$;

$Qb = Qb + (x(i) * hb(i, 1/deltat + 1) * dx/sqrt(h0 * kappaC))$;

$Qc = Qc + (x(i) * epsilon * hc(i, 1/deltat + 1) * dx/sqrt(h0 * kappaC))$;

$Qhomo = Qhomo + (x(i) * u(i, 1/deltat + 1) * dx/sqrt(h0 * kappaC))$;

$U(i, 1) = u(i, 1/deltat + 1)$; % Update the initial state of homoporous blocks

$H_B(i, 1) = hb(i, 1/deltat + 1)$; % Update the initial state of porous blocks

$H_C(i, 1) = hc(i, 1/deltat + 1)$; % Update the initial of the system cracks

end

plot(x,U(:,1))
title('Profile purely H at initial')
xlabel('x')
ylabel('H')
axis ([0 10 0 1])
pause
plot(x,$H_B(:, 1)$)
title('Profile$H_B$at initial')
xlabel('x')
ylabel('H')
axis ([0 10 0 1])
pause
plot(x,$H_C(:, 1)$)
title('Profile $H_C$at initial')
xlabel('x')
ylabel('H')
axis ([0 10 0 0.001])
pause
%%%%%%%%%%%%
% the numerical schemes %
%%%%%%%%%%%%
for k=1:Ntime % Time Loop
for i=2:N % Space Loop

$H_B(i,k+1) = H_B(i,k) + sB * (H_B(i-1,k).^2 + H_B(i+1,k).^2 - 2. * H_B(i,k).^2) - dt * (H_B(i,k).^2 - H_C(i,k).^2) * beta;$

$H_C(i,k+1) = H_C(i,k) + sC * (H_C(i-1,k).^2 + H_C(i+1,k).^2 - 2. * H_C(i,k).^2) + dt * (H_B(i,k).^2 - H_C(i,k).^2) * (beta/epsilon);$

$U(i,k+1) = U(i,k) + s*(U(i-1,k).^2 + U(i+1,k).^2 - 2.*U(i,k).^2) - dt * (H_B(i,k).^2) * beta;$

end

$H_B(1,k) = 0;$
$H_B(N+1,k) = 0;$
$H_C(1,k) = 0;$
$H_C(N+1,k) = 0;$
$U(1,k) = 0;$
$U(N+1,k) = 0.;$
end

%————————dipole moment————————————

density=997; $\%kg/m^3$
qtime=-1:dt:T;
qstarb=-0.95;

for q=1:Ntime+1
if $qtime(q) < qstarb$
$qb(q) = (Qb + f(q) * x(i) * dx)/(kappaC * h0^2);$
else
$qb(q) = Qb;$
end
$mass_b(q) = Qb * density;$
end

$qstarc = 0;$

for $q = 1 : Ntime + 1$
if$qtime(q) < qstarc$
$qc(q) = (Qc + epsilon * f(q) * x(i) * dx)/(kappaC);$
else
$qc(q) = Qc;$

end
$mass_c(q) = Qc * density;$
end

figure(1)
semilogy(time,qb,'- -',time,qc)
grid on
title('Dipole moment')
xlabel('Θ')
ylabel('Q')
legend('porous blocks','cracks')
axis([-1 10 $10^{(-12)}$ $10^{(-4)}$])

figure(2)
semilogy($time, mass_c, time, mass_b$,'- -')
grid on
title('Fluid mass')
xlabel('Θ')
ylabel('Mass')
legend('cracks','porous blocks')
axis ([0 1000 $10^{(-6)}$ $10^{(-1)}$])

pause

% front position %

%purely porous blocks

for $k = 1 : Ntime + 1$
$xf_{pure}(k) = 2 * (5 * Qhomo * time(k))(1/4);$
$x_f{}^*(k) = 2 * (5 * (Qb - Qc) * time(k))(1/4);$
end

% Fissurized porous blocks
$xf0 = 34.0$; % front at initial t=0
$V = 2 * 1e - 03$; % dimensionless velocity of the front

for $k = 1 : Ntime + 1$
$xf_{frac}(k) = xf0 + V * time(k) * sqrt(h0 * kappaC);$
end

```
        figure(3)
semilogy(time,xf_pure,time,xf_frac,'- -',time,x_f*,':')
title('Front position x_f(t)')
xlabel('Θ')
ylabel('x')
legend('purely porous blocks','Fissurized porous blocks','x_f*')
axis ([0 1000 10^(-2) 10^(2)])

        pause

        %————plot the results————————————
        K1=1002; K2=10002; K3=100002;

        figure(1)
plot(x,H_C(:,K1),x,H_B(:,K1),'- -')
title('Numerical solution at t=10')
xlabel('x')
ylabel('H')
axis ([0 10 0 0.01])
legend('cracks','porous blocks')

        figure(2)
plot(x,H_C(:,K2),x,H_B(:,K2),'- -')
title('Numerical solution at t=100')
xlabel('x')
ylabel('H')
axis([0 10 0 0.01])
legend('cracks','porous blocks')

        figure(3)
plot(x,U(:,K3),'-.',x,H_C(:,K3),x,H_B(:,K3),'- -')
title('Numerical solution at t=1000')
xlabel('x')
ylabel('H')
axis([0 10 0 0.01])
legend('purely porous blocks','cracks','porous blocks')
```